NASA Technical Memorandum 107030
AIAA–87–1814

Comparison of Fusion/Antiproton Propulsion Systems for Interplanetary Travel

Stanley K. Borowski
Lewis Research Center
Cleveland, Ohio

Prepared for the
23rd Joint Propulsion Conference
cosponsored by AIAA, ASME, SAE, and ASEE
San Diego, California, June 29—July 2, 1987

National Aeronautics and
Space Administration

Comparison of Fusion/Antiproton Propulsion Systems for Interplanetary Travel

Stanley K. Borowski*
National Aeronautics and Space Administration
Lewis Research Center
Cleveland, Ohio 44135

Abstract

Rocket propulsion driven by either thermonuclear fusion or antiproton annihilation reactions is an attractive concept because of the large amount of energy released from a small amount of fuel. Charged particles produced in both reactions can be manipulated electromagnetically making high thrust/high specific impulse (I_{sp}) operation possible. A comparison of the physics, engineering, and costs issues involved in using these advanced nuclear fuels is presented. Because of the unstable nature of the antiproton-proton ($\bar{p}p$) reaction products, annihilation energy must be converted to propulsive energy quickly. Antimatter thermal rockets based on solid and liquid fission core engine designs offer the potential for high thrust (~10^5 lbf)/high I_{sp} (up to ~2000 s) operation and 6 month round trip missions to Mars. The coupling of annihilation energy into a high-temperature gaseous or plasma working fluid appears more difficult, however, and requires the use of heavily shielded superconducting coils and space radiators for dissipating unused gamma ray power. By contrast, low-neutron-producing advanced fusion fuels (Cat-DD or DHe^3) produce mainly stable hydrogen and helium reaction products which thermalize quickly in the bulk plasma. The energetic plasma can be exhausted directly at high I_{sp} ($\simeq 10^5$s) or mixed with additional hydrogen for thrust augmentation. Magnetic fusion rockets with specific powers (α_p) in the range of 2.5 to 10 kW/kg and I_{sp} in the range of 20,000–50,000 s could enable round trip missions to Jupiter in less than a year. Inertial fusion rockets with $\alpha_p > 100$ kW/kg and $I_{sp} > 10^5$s could perform round trip missions to Pluto in less than 2 years. On the basis of preliminary fuel cost and mission analyses, fusion systems appear to outperform the antimatter engines for difficult interplanetary missions.

Introduction

A high-performance rocket system must operate with both a high-specific impulse I_{sp} and a low-mass powerplant (M_W) capable of generating large amounts of jet power (P_{jet}). Because the thrust-to-engine weight ratio [F(kg)/M_W(kg) = 2000 α_p (kW/kg)/ g_o^2 I_{sp} (s)] of a spacecraft is directly proportional to the engine specific power ($\alpha_p \equiv P_{jet}/M_W$), large values of α_p are required to provide the acceleration levels necessary for rapid transportation of cargo and personnel throughout the solar system. An analysis of the yield from various energy sources (Table 1) indicates that only the nuclear fuels (fission, fusion, and synthetic antihydrogen fuels) can provide the power requirements for tomorrow's high-thrust/high-I_{sp} space drives.

For convenient interplanetary travel to become a reality, propulsion systems capable of operating in the middle to upper right portion of the P_{jet} vs I_{sp} plane (shown in Fig. 1) are required. Classical chemical (C) propulsion systems (occupying the left-hand side of Fig. 1) have a high-specific power capability [$\alpha_p \simeq 1550$ kW/kg for the Space Shuttle main engine (SSME)] but the power per unit mass of ejected matter is small (i.e., these systems operate at low I_{sp}) and great quantities of propellant are needed to essentially push propellant around. Electric propulsion (EP) systems use power from an onboard nuclear power source to accelerate propellant to high-exhaust velocities ($I_{sp} = 10^3$–10^4 s). However, the added weight of the power conversion and heat rejection systems and the efficiency toll of multiple energy conversion processes result in a low-specific power (~0.1 kW/kg) and restrict EP systems to low-thrust operation. Their high payload mass fraction capability can be exploited, however, for deep interplanetary or cargo transport missions.

Direct thrust nuclear propulsion systems (based on increasingly more sophisticated forms of nuclear energy conversion) provide the means of accessing the high-thrust/high-I_{sp} area of parameter space. Solid core fission thermal rockets (SCR) use the thermal energy released in the fission process to heat a working fluid (typically hydrogen), which is then exhausted to provide propulsive thrust. The SCR has a specific impulse potential comparable to the electrothermal (ET) thruster (~10^3 s) yet delivers thrust levels equivalent to those of chemical engines (~10^5 lbf). The performance of the SCR is limited, however, by the melting temperature of the fuel, moderator, and core structural

*Work performed while author was with Aerojet Propulsion Research Institute, 1987.

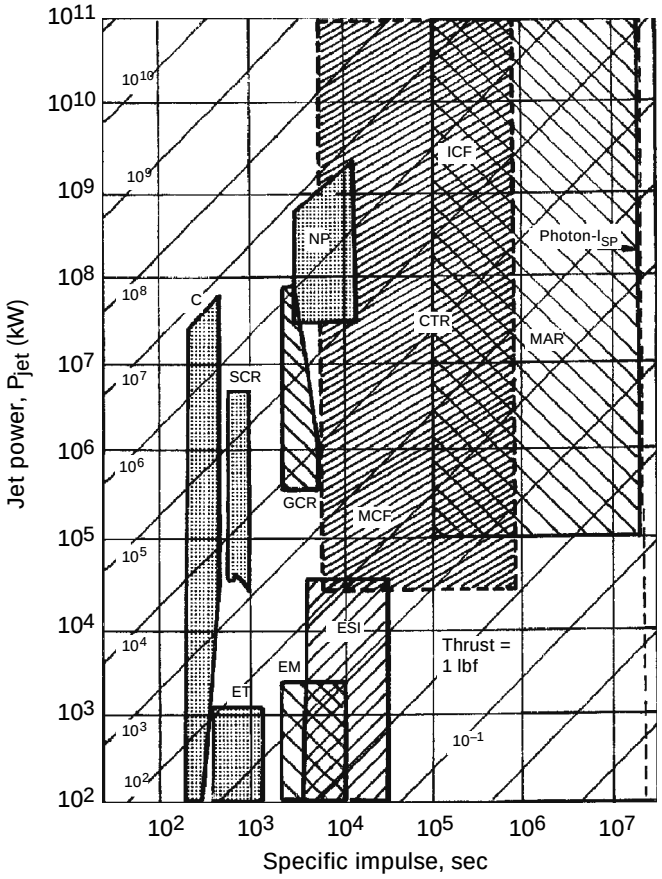

Figure 1.—Fusion and antimatter engines offer possible performance capabilities over a wide range of parameters.

materials. By operating the fuel in a high-temperature fissioning plasma state, the gaseous core thermal rocket (GCR) can exhaust propellant at substantially higher values of specific impulse [in the range of electromagnetic (EM) and electrostatic ion (ESI) thrusters ~ 3000–6000 s].

Still higher values of I_{sp} (~5000–10^6 s) are possible with controlled thermonuclear fusion rockets (CTR). Fusion systems based on magnetic and inertial confinement fusion (MCF and ICF) can bridge the gap between fission systems (examples of which are the nuclear-electric, nuclear-thermal, and nuclear-pulsed (NP) Orion type concepts shown in Fig. 1), and the relativistic mass annihilation rocket (MAR) of the more distant future. An examination of the various possible MAR configurations[1,2] indicates that antimatter propulsion need not be restricted to the purely relativistic range of exhaust velocities shown in Fig. 1. In fact, in the studies reported thus far, there is a heavy reliance on the concepts and technologies presently being developed in our nation's fission and fusion research programs. This should not be too surprising, however, because fission and fusion reactors are annihilation engines in their own right [albeit inefficient in terms of the total mass fraction converted to energy (see Table 1)].

Nuclear propulsion is currently receiving greater attention by both NASA and the U.S. Air Force. In Refs. 3 and 4, the Air Force has identified the direct fission thermal rocket and the antiproton annihilation engine (MAR) as systems worthy of development. The interest in antimatter is attributed to the fact that it is a highly concentrated form of energy storage (see Table 1). A milligram of antihydrogen $\bar{H}$ [consisting of an antiproton $\bar{p}$ and a positron e^+ (an antielectron)] reacted totally with the same amount of normal hydrogen possesses an energy content equivalent to ~ 13 t (1 metric ton (t) = 10^3 kg) of LO_2/LH_2. Although synthetic $\bar{H}$ is definitely a "high-test" propellant, it requires a large energy investment and will be expensive to manufacture (~\$$10^{10}$/g assuming commercial electricity usage[5]), and difficult to store and manipulate. Estimates by Howe et al.[6] indicate that a production facility capable of generating a gram of antiprotons per year (~1.9×10^{16} $\bar{p}$/s assuming continuous year round operation) could be possible by the year 2010 on the basis of antiproton production extrapolations. Assuming an overall energy efficiency of ~2.5×10^{-4} (Ref. 7) (a factor of ~10^4 improvement over current Fermilab capabilities), the power requirements necessary to drive a 50% efficient production accelerator would be ~45 GW; 1 GW = 10^9 W (equivalent to the total power output of ~15 commercial nuclear power plants).

In addition to the cost and production issues, when one considers the technological complexities of annihilation engines involving 1) antiproton storage, extraction, and injection, 2) magnet and cargo shielding against copious amounts of penetrating gamma radiation, and 3) the conversion of "unstable" and very energetic charged reaction products to thrust, it appears that fusion systems could offer substantial advantages over antimatter systems. These advantages include 1) proven fueling, heating, and confinement techniques, 2) stable hydrogen and helium reaction products, and 3) an abundant fuel supply.

The purpose of this chapter is to compare various antimatter and fusion rocket designs in an effort to obtain a clearer understanding and potentially quantify the advantages and disadvantages of each system. The areas examined will include mission capability, fuel costs and availability, and technology requirements. In Sec. II, the characteristics of the $\bar{p}p$ reaction and the various fusion fuel cycles are presented. Some of the issues touched on include the energy yield per reaction and its distribution among charged particles, neutrons, and gamma radiation, and the requirements on engine design of utilizing stable vs unstable reaction products for propulsive purposes. In Sec. III a variety of antimatter and fusion propulsion concepts are described. Comparisons are also made between the different MAR configurations and their fission/fusion analog. Simple weight estimates and engine performance parameters are presented and used in a mission performance analysis, the results of which are found in Sec. IV. A summary of findings and the conclusions drawn from them are presented in Sec. V.

Table 1 Yield from various energy sources

Fuels	Reaction products	Energy release, J/kg	Converted mass fraction
		$(E/m_i = \alpha c^2)$	$\left(\alpha \equiv \frac{\Delta m}{m_i} = \frac{m_i - m_f}{m_i}\right)$[a]
Chemical:			
Conventional: (LO_2/LH_2)	water, hydrogen,	1.35×10^{7}	1.5×10^{-10}
Exotics: atomic hydrogen,	common hydrogen,	2.18×10^{8}	2.4×10^{-9}
metastable helium	helium (He^4)	4.77×10^{8}	5.3×10^{-9}
Nuclear fission[b]:			
U^{233}, U^{235}, Pu^{239} (~200Mev/U^{235} fission)	radioactive fission fragments, neutrons, γ-Rays	8.2×10^{13}	9.1×10^{-4}
Nuclear fusion[c]:			
DT (0.4/0.6)	helium, neutrons	3.38×10^{14}	3.75×10^{-3}
Cat-DD(1.0)	hydrogen, helium, neutrons	3.45×10^{14}	3.84×10^{-3}
DHe^3 (0.4/0.6)	hydrogen, helium (some neutrons)	3.52×10^{14}	3.9×10^{-3}
pB^{11} (0.1/0.9)	helium (thermonuclear fission)	7.32×10^{13}	8.1×10^{-4}
Matter plus antimatter[d]:	Annihilation radiation		
$\bar{p}p$ (0.5/0.5)	pions, muons, electrons, positrons → Neutrinos and γ rays	9×10^{16}	1.0

[a] Δm is the change in mass between reactants (m_i) and products (m_f).
[b] U^{233}, U^{235}, Pu^{239} are fissile isotopes of uranium and plutonium.
[c] Weight composition corresponds to a 50/50 fusion fuel mixture; Cat-DD is the catalyzed DD reaction enhanced by burnup of reaction tritons (T) and helium-3 (He^3) nuclei with deuterons (D) in situ; B^{11} is the fusionable isotope of boron.
[d] Proton and Antiproton indicated by p, $\bar{p}$.

Considerations in the Use of Antiproton and Fusion Fuels

The energy content, reactivity, portability, availability, and practicality (in terms of charged particle output) are important considerations in the preliminary design of possible antiproton and fusion propulsion systems. A large energy yield per reaction or per kilogram of fuel is valuable only if it can be effectively used for propulsive thrust. Whereas antihydrogen fuel has a specific energy (E_{sp}) ~10^3 times that of fission and ~10^2 times that of fusion, this parameter can be misleading when viewed within the context of an actual propulsion system. For example, the fission process (Esp ~8.2×1013 J/kg) has a theoretical maximum specific impulse [Isp = (2 Esp/ g_o^2)1/2] of ~1.25×106s (assuming all of the fissionable mass is available for thrust generation). This is not the case in real reactor engine system, however, where the energy liberated in the fission process appears as heat in the reactor fuel rods. The core assembly is maintained at temperatures compatible with structural

requirements by flowing liquid hydrogen through the reactor. In the NERVA nuclear rocket engine[8] hydrogen temperatures of ~2500 K at the nozzle entrance led to I_{sp} values of ~825 s. [Unlike the solid fission core reactors, in a magnetic fusion rocket engine the fusion fuel exits in a high-temperature plasma state and plasma power can be extracted using a magnetic diverter/nozzle configuration (discussed in Sec. III).] Whereas the I_{sp} of fission engines can be improved significantly by going to a gaseous fission core system[9], in the case of a solid core engine, technology limitations effectively reduce the specific energy of the fission fuel to ~3×10^7 J/kg - only a factor of ~2 better than LO_2/LH_2. In addition to the constraints imposed on engine design by the available technology, hardware requirements for storage, extraction and injection of hard-to-handle cryogenic and/or exotic fuel supplies can lead to excessive weight penalties (in terms of refrigeration mass, complex electromagnetic containers and transfer conduits, shielding, etc.) that may further degrade the perceived benefits of the fuel source.

Fusion Fuels

Table 2 shows the energy release and the reaction products associated with the various nuclear fuels. In the fission process a heavy uranium nucleus such as U^{235} is split into two fragments

Table 2 Released energy and products from various nuclear reactions

Typical fission :

$$_{92}U^{235} + {}_0n^1 \rightarrow {}_{56}Ba^{137} + {}_{36}Kr^{97} + 2\,{}_0n^1 + \Delta E \ (\approx 200\ \text{MeV})$$

Fusion :

$${}_1D^2 + {}_1D^2 \xrightarrow{50\%} {}_1T^3 + {}_1p^1 + \Delta E \ (= 4.03\ \text{MeV}) \ \text{proton branch}$$

$$\xrightarrow{50\%} {}_2He^3 + {}_0n^1 + \Delta E \ (3.27\ \text{MeV}) \ \text{neutron branch}$$

$${}_1D^2 + {}_1T^3 \rightarrow {}_2He^4 + {}_0n^1 + \Delta E \ (= 17.6\ \text{MeV})$$

$${}_1D^2 + {}_2He^3 \rightarrow {}_2He^4 + {}_1p^1 + \Delta E \ (= 18.3\ \text{MeV})$$

$$6\,{}_1D^2 \rightarrow 2\,{}_2He^4 + 2\,{}_1p^1 + 2\,{}_0n^1 \ (\Delta E = 43.2\ \text{MeV}) \ \text{catalyzed–DD}$$

100% burnup of T and He^3 with D

$${}_1p^1 + {}_5B^{11} \rightarrow 3\,{}_2He^4 + \Delta E \ (= 8.7\ \text{MeV}) \ \text{thermonuclear fission}$$

$\bar{p}p$ Annihilation :

$$\bar{p} + p \rightarrow m\pi^0 + n\pi^+ + n\pi^- + \Delta E \ (\approx 1213\ \text{MeV}); \text{m} = \text{n} \approx 1.6$$

$$\pi^0 \xrightarrow{84\ \text{as}^a} 2\gamma \ (E_\gamma \approx 200\ \text{MeV})$$

$$\pi^+ \xrightarrow{70\ \text{ns}^b} \mu^+ + \nu_\mu \ (\text{muon neutrino})$$

$$\pi^- \xrightarrow{70\ \text{ns}} \mu^- + \bar{\nu}_\mu$$

$$\mu^- \xrightarrow{6.2\ \mu\text{s}^c} e^- + \nu_\mu + \bar{\nu}_e \ (\text{electron antineutrino})$$

$$\mu^+ \xrightarrow{6.2\ \mu\text{s}} e^+ + \nu_e + \bar{\nu}_\mu$$

$$e^- + e^+ \rightarrow 2\gamma \ (E_\gamma = 0.511\ \text{MeV})$$

[a]Attosecond = 10^{-18} s.
[b]Nanosecond = 10^{-9} s.
[c]Microsecond = 10^{-6} s.

with a release of considerable energy and the emission of neutrons and gamma rays. Energy can also be generated by fusing together light elements provided the temperature of the ionized mixture is sufficiently high (on the order of ~10^8–10^9 K) for the positively charged fuel ions to overcome their coulomb repulsion. The fuel cycles with the greatest reactivity at temperatures below 100 KeV (1 keV = 1.16×10^7 K) involve the hydrogen isotopes deuterium D and tritium T and the helium isotope He^3. The energy liberated in the fusion process is partitioned among the reaction products (which includes neutrons *n*, hydrogen *p* and helium He^4) and appears in the form of kinetic energy. The DT cycle has the largest reaction rate at low temperatures (≤15 keV). Unfortunately it releases 80% of its energy in energetic (14.1 MeV) neutrons which can only be recovered in a complex tritium breeding blanket structure using thermal conversion equipment. Substantial quantities of shielding are also required for protection of crew and equipment (primarily the superconducting coils used to generate the plasma confining magnetic fields). The excessive weights involved in using DT appear to rule out its use for propulsion systems.

The DD fusion reaction is characterized by two branches (a neutron and a proton branch) which occur with roughly equal probability. By burning the tritium and He^3 resulting from these energy-poor reactions in the DD plasma itself, a catalyzed DD (Cat-DD) burn results, which has a significantly improved energy output (~14.4 MeV/pair of DD fuel ions burned). In addition, greater than 60% of the energy output from a Cat-DD reactor appears in the form of charged particles (protons and He^4). The attractiveness of the Cat-DD fuel cycle is that it is self-sufficient, i.e., it requires only naturally available deuterium as the main fuel feed. It is also relatively inexpensive (~$\$10^3$/kg) (Ref. 10) and abundant (estimates of the deuterium content in the Earth's oceans and surface waters are placed at ~10^{13} t).

The DHe^3 reaction is particularly attractive for propulsion application and has the largest power density of all of the advanced fusion fuels over the temperature range of ~45−100 keV. Neither of the fuel components are radioactive, and both of the reaction products that is, a 14.7-MeV proton and a 3.6-MeV He^4 nuclei or alpha particle, are charged making magnetic extraction and thrust generation possible. The charged plasma can be either exhausted directly at high I_{sp} (~10^5–10^6 s) or mixed with additional hydrogen reaction mass in a bundle diverter/magnetic nozzle for thrust augmentation at lower I_{sp} (≳10^4 s). This interchangeability of thrust and I_{sp} is one of the potential operational advantages of fusion propulsion.

In addition to its relative cleanliness (<5% neutron power produced via DD side reactions), the DHe^3 cycle has an appreciable energy yield, i.e., a kilogram of DHe^3 (with a 50/50 weight composition) produces ~25×10^6 times more energy than a kilogram of LO_2/LH_2. Until recently, the problem with the DHe^3 cycle has been the lack of abundant natural He^3 on Earth. This has changed with the identification of a potentially abundant source (~10^9 kg) of He^3 deposited on the lunar surface by solar wind bombardment.[11] It is estimated that this reserve could provide adequate He^3 for both propulsion and power production for many decades or until such time as the vast reserves (~10^{23} kg) of He^3 from Jupiter can be tapped.[11]

A final item of significance which could impact future DHe^3 usage deals with recent theoretical and experimental work[12,13] on the use of spin-polarized fusion fuels. Indications are that spin polarization of the DHe^3 nuclei (prior to reactor injection) can enhance the fuel's reactivity by 50% while simultaneously suppressing the troublesome neutron-producing DD side reactions. If the perceived benefits of spin polarized fuel are borne out in the future a clean, fusion-powered, manned planetary transportation system could be available in the first half of the 21st century. Finally, on a longer time scale the proton-based pB^{11} (boron-11 isotope) fuel cycle could lead to a superclean fusion engine which exhausts only helium-4 nuclei produced by a fusion reaction which is equivalent to thermonuclear fission.

Antiproton Annihilation

In contrast to the positron–electron (e^+e^-) reaction which emits two 0.511-MeV gamma rays, the antiproton–proton ($\bar{p}p$) reaction shown in Table 2 releases its considerable energy content (~1876 MeV/annihilation) primarily in the form of relativistic neutral and charged pions (or π mesons). Each pion possesses an average total energy [$E_t = E_0 + \Delta E = \gamma E_0$; $\gamma = 1 + (\Delta E/E_0)$] of ~390 MeV which consists of the particle's rest mass E_0 and kinetic energy ΔE components. The charged pions carry either a unit positive (π^+) or negative (π^-) electron charge and each has a rest mass energy of ~140 MeV. The neutral pion (π^0) has zero electric charge and is slightly lighter at ~135 MeV. With roughly 1.6 of each type of pion being produced per annihilation, the total kinetic and rest mass energies attributed to all pions is ~1212 MeV and 664 MeV, respectively.

Because the pion reaction products are unstable, several decay chains occur before the fuel mass is converted totally to energy. The neutral pion decays almost immediately into two high-energy gamma rays each with an average energy of ~200 MeV. The generation of gamma-ray power will be substantial in an MAR and represents about one-third of the energy released in the $\bar{p}p$ reaction. The charged pions, with a relativistic mean lifetime ($t = \gamma t_0$, $t_0 = 26$ ns) of ~70 ns, decay into neutrinos and unstable charged muons (E_0 ~ 106 MeV). Cassenti[14] has estimated the distribution of energy among the muons and neutrinos following the decay of the charged pions in vacuum. His results indicate that the neutrinos carry off ~22% of the available pion energy (~1248 MeV) whereas the muons retain ~78%. The unstable muon, having an average energy of ~300 MeV, also decays (in ~6.2 μs) into an electron, or positron, and two neutrinos as shown in Table 2. The energy appears to be about equally distributed among the three particles with the neutrinos carrying off ~2/3 of the available energy. Ultimately, the

electrons and positrons can also annihilate yielding additional energy in the form of two 0.511- MeV gamma rays. The neutrinos are considered to be massless and move at essentially the speed of light. They are extremely penetrating and rarely interact with matter. Under vacuum conditions the various muon and electron neutrino particle–antiparticle pairs carry off ~50% of the available annihilation energy following a $\bar{p}p$ reaction.

The designer of antiproton propulsion systems, aware of this annihilation history, must device reactor/rocket engine configurations capable of 1) utilizing the tremendous energy content of the $\bar{p}p$ reaction products and 2) effectively accessing that range of exhaust velocities required for a particular mission. Because each π^0 meson decays almost immediately into two gamma rays, the particles which must be dealt with for thrust generation include 1) the high-energy charged pions (both the π^+ meson and its antiparticle, the π^- meson), 2) the generations of decay charged particles which follow (muons, electrons, and positrons), and 3) 200-MeV gamma rays. The charged particles can be either exhausted directly at high I_{sp} using a magnetic nozzle as discussed by Morgan,[15] or they can be trapped in a magnetic container and their kinetic energy used to heat a working propellant[15,16] for lower I_{sp} operation.

To put the energy in the charged pions to use for direct propulsive thrust, an axially diverging magnetic nozzle configuration can be employed to convert the perpendicular energy of the charged pions to directed energy along the nozzle axis. At a kinetic energy of 250 MeV, the directed pions will exit the nozzle at an exhaust velocity of $v_{ex} \simeq 0.94c$ (corresponding to a $I_{sp} \simeq 28.8\times10^6$ s). Assuming engine operation at the 100-lbf thrust level, the corresponding jet power is P_{jet} (= $Fv_{ex}/2$) $\simeq$ 62.7 GW. Associating this power level with the charged pion exhaust (~2/3 of the total generated annihilation power), one finds that ~31.4 GW (~2.7×10^{10} Ci) of 200-MeV gamma-ray power is also being generated. Shielding sensitive spacecraft components (such as crew, ship electronics, and both cryogenic and superconducting coil systems for the magnetic nozzle) against this level of radiation and dissipating the heat appears impossible.

Depending on power level, the decay gamma energy can be recovered for propulsive purposes using a regeneratively cooled tungsten shield. Hydrogen flowing through channels in the shield and exiting at the nozzle throat could provide cooling for both components, as well as a source of hot hydrogen for thrust augmentation. However, the exclusive reliance on this open-cycle coolant mode deprives the antimatter rocket of one of its operational advantages, namely, the wide range of interchangeability of thrust and specific impulse. Operational flexibility can be maintained by employing a closed-cooling cycle space radiator system (discussed in Sec. III) capable of responding to thrust variations by varying the number of primary radiator modules in use. With such a system, an adequate cooling level is possible even during high I_{sp} operation when the hydrogen flow is reduced.

Specific impulse values more appropriate for interplanetary travel (~5000– 20,000 s) should be possible by allowing the charged pions to transfer their kinetic energy collisionally to a working gas. The resulting exhaust would have nearly the same energy content as the charged pion exhaust (assuming negligible losses for dissociation and ionization) but would generate increased levels of thrust due to the higher mass throughout. To achieve collisional coupling, the slowing down or stopping time of the charged pions in the working gas/plasma must be less than the pions mean life time. If the charged pions or muons decay before dissipating an appreciable percentage of their kinetic energy into the host gas/plasma, an increasing portion of the available annihilation energy will be lost in the form of unrecoverable neutrinos. This dissipation process is not trivial. As an example, we consider an antimatter rocket with a hydrogen working gas and a reaction chamber pressure and temperature of 200 atm (1 atm = 1.013×10^5 newtons) and 3000 K (corresponding to an I_{sp} ~1000 s). At these conditions the density ρ of H_2 is ~1.63×10^{-3} g/cm^3. The corresponding range of a 250-MeV charged pion is ~47.1 g/cm$^2/\rho \simeq$ 290 m (Ref. 17) and the stopping time (~$\Delta\bar{E}_\pi/SP\cdot\rho\cdot\bar{v}$) is ~0.3 μs (~130 μs at 2000 atm). Here *SP* is the stopping power in MeV-cm^2/g (Ref. 17), and $\bar{v}$ is the average velocity of the charged pion. These values are orders of magnitude larger than the mean range and lifetime of the pion in vacuum. As a result, magnetic fields will be required to contain the energetic charged pions (and muons) within the reaction chamber, and superconducting magnets (requiring negligible recirculation power) will be a critical component of the annihilation engine design. Finally, because the average kinetic energy of a charged pion is roughly a factor of 20 larger than that of the most energetic fusion reaction product (a 14.7-MeV proton from the DHe^3 reaction), the pion gyroradius, given (in mks units) by

$$r_{gyro}(m) = \left(\gamma^2 - 1\right)^{1/2}\left[m_\pi c/eB(T)\right] \qquad (1)$$

will be more than twice that of the proton for a given magnetic field strength *B*. [The parameters *c* and *e* are the speed of light and the electron charge (1.602×10^{-19} C), respectively.] To ensure adequate containment in antimatter rocket engines, magnetic field strengths higher than those currently being contemplated for use in fusion reactors will be needed.

Fusion and Antiproton Propulsion Concepts

Rocket propulsion driven by thermonuclear fusion or antiproton annihilation reactions is an attractive concept: a large amount of energy can be released from a relatively small amount of fuel, and the charged reaction products can be manipulated

electromagnetically for thrust generation. Propulsion systems deriving their energy from these high-energy density fuels have the potential to simultaneously demonstrate large exhaust velocities and high jet power levels. However, these advanced propulsion reactors will be quite complex and must be designed to be portable, compact, and self-contained. This set of criteria will necessitate the development of lightweight reactor/driver systems, radiation shields, high current density superconductors, cryoplants for magnet/propellant maintenance, power conversion equipment for reactor startup and operating support, heat rejection systems for waste heat, magnetic nozzle designs for thrust generation, and structure for reactor support and spacecraft integration. In the case of antiproton fuel, complex electromagnetic containers and conduits will be required for storage, extraction and injection of this volatile fuel. Fortunately, a major component of a fusion (and possible an antiproton) power plant, namely, the vacuum pumping system, should be considerably simplified for space-borne reactors.

Magnetic Confinement Fusion

Fusion reactors based on the magnetic confinement concept use superconducting coils to generate the strong magnetic fields needed to confine and isolate the ultrahot power-producing plasma from the reaction chamber walls. The fusion plasma, consisting of positively charged fuel ions and negatively charged free electrons, has a kinetic pressure which can be expressed as a percentage of the confining magnetic field pressure through the use of the local plasma beta value, β defined (in mks units) by

$$\beta = \frac{n_e k\, T_e + n_i k\, T_i}{B^2/2\mu_o} \qquad (2)$$

The parameters $n_{e(i)}$, $T_{e(i)}$, and B are the electron (ion) particle density, temperature (in kiloelectronvolts keV), and magnetic field strength, respectively. The constant $k = 1.602\times10^{-16}$ J/keV and μ_o is the permeability of free space. The power density in a fusion reactor is given by

$$P_f/V_p = \alpha_{jk} n_j n_k \left\langle \sigma_{jk} v \right\rangle k Q_{jk}; \quad \alpha_{jk} = \begin{Bmatrix} 1; & j \neq k \\ 1/2; & j = k \end{Bmatrix} \qquad (3)$$

where P_f and V_p are the fusion power and plasma volume, $n_{j,k}$ are the respective densities of the two reacting ion species, $\langle\sigma v\rangle$ is the maxwellian-averaged fusion reactivity (Fig. 2) and Q_{jk} is the energy release per jk reaction (appears as ΔE in Table 2). Assuming $n_e = n_i$, $T_e = T_i$, $\alpha_{jk} = 1$ and $n_j = n_k = n_i/2$ (a 50/50 fuel mix), Eq. (3) can be rewritten as

$$P_f/V_p = k' \;\; \beta^2 B^4 \left[\left\langle \sigma_{jk} v \right\rangle \Big/ T_i^2 \right] Q_{jk} \qquad (4)$$

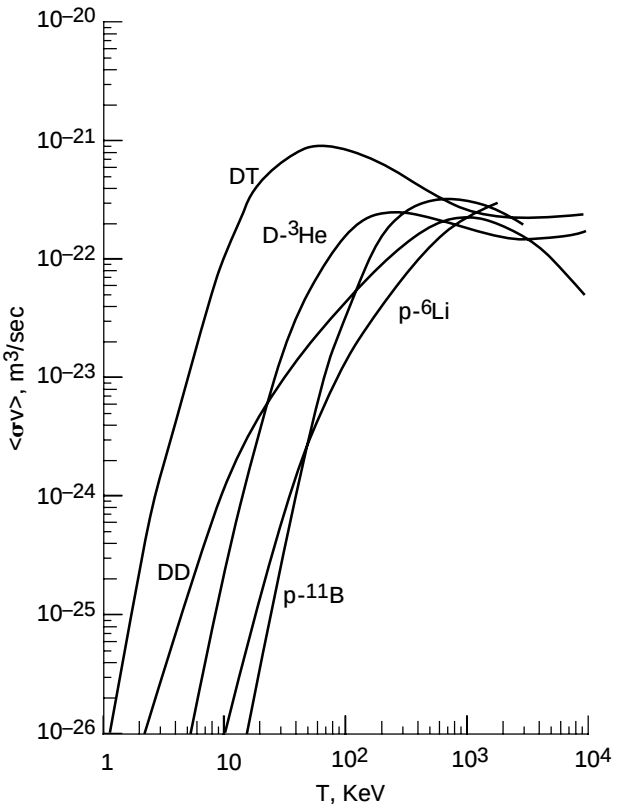

Figure 2.—A comparison of DT and advanced fuel reactivities.

where $k' \approx 6.18\times10^{25}$. Equation (4) shows that for a maximum magnetic field strength capability and optimal operating temperature (where $\langle\sigma v\rangle/T_i^2$ is a maximum), the fusion power density scales like β^2. There is, therefore, a strong incentive to develop MCF concepts that can operate at high β. Two candidate MCF systems which could be developed for propulsion applications are the spherical torus (ST) advanced tokamak concept[18] and the Spheromak compact toroid configuration.[19]

Spherical Torus Tokamak

The ST is a low-aspect-ratio version of the Tokamak concept currently the world standard for magnetic confinement fusion research. The aspect ratio A ($\equiv R_o/a$) is 1.5–2.0 in the ST (~4 in a conventional tokamak), R_o being the major radius of the torus and a the plasma minor radius. As shown in Fig. 3, the ST is a toroidal device consisting of a hollow vacuum vessel used for the production and confinement of large volumes of high-temperature plasma. The donut-shaped plasma is immersed in a helically twisted magnetic field formed through the combination of a toroidal field (produced by a set of toroidal field coils which wrap around the torus) and a poloidal field component (produced by a current flowing through the plasma itself). In a large-aspect-ratio tokamak $B_t >> B_p$, but in the spherical torus

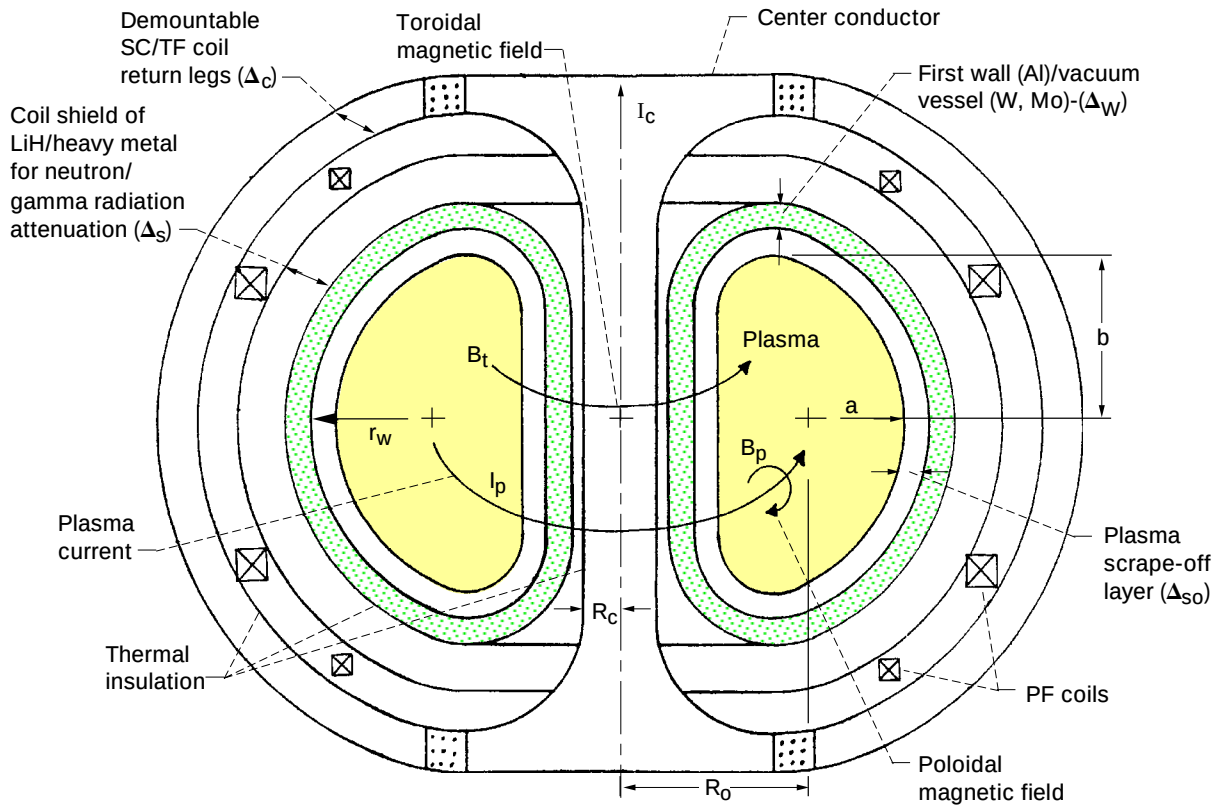

Figure 3.—Schematic of an advanced (spherical torus) tokamak reactor system.[21]

B_p can be comparable to B_t at the plasma outboard edge. Also, because of the large poloidal current component of I_p, plasma enhancement of the on-axis toroidal field (referred to as paramagnetism) is significant in the ST (a factor of ~2 larger than the vacuum field generated by the TF coils). Because of the ST's small aspect ratio, high-β operation is possible, however, standard inductive current startup techniques are difficult and efficient noninductive current drive techniques are required.[20] A cross section of the ST's magnetic field structure yields a set of nested poloidal magnetic field surfaces which exhibit toroidal symmetry. It is on these surfaces that the circulating hot-plasma particles are confined and across which they conduct heat and collisionally diffuse. By injecting supplementary heating (either as beams of energetic neutral atoms or as wave energy), the plasma temperature can be increased to the point where the plasma ignites, i.e., its reactivity is sufficiently high that the power of the charged fusion reaction products (P_{cp}) alone can maintain the fusioning plasma temperature against losses associated with radiation [both bremsstrahlung (P_{brems}) and synchroton (P_{synch})] and transport mechanisms. Exhausting this transport power P_{tr} for thrust generation and thermally converting the radiation loss (which can also include neutron radiation) for needed recirculation power are the key elements of a self-sustaining magnetic fusion rocket (see Fig. 4).

In terrestrial power reactor designs of the ST burning DT fuel only what is absolutely indispensable inboard of the plasma is retained. This includes a first wall/vacuum chamber arrangement and a normal center conductor that carries current to produce the tokamak's magnetic field. Other components, such as the solenoidal and inboard neutron shielding, are eliminated. The resulting devices have exceptionally small aspect ratios ($1.3 \sim A \sim 2.0$) and, in appearance look much like a sphere with a modest hole through the center, hence, the name spherical torus.

The potential for neutronless fusion power generation made possible through the use of spin-polarized DHe^3 has led to the examination of a high field ($B_t \sim 10$ T), superconducting version of the ST for rocket application.[21] The configuration is illustrated in Fig. 3 where we have speculated on the possibility of using demountable SC/TF coil legs to improve access to the internal torus and poloidal field coils. The central conductor is assumed to use a high field/high current density ($\leq 10^8$ A/m^2) superconductor employing an advanced vanadium–gallium alloy (V_3Ga) and an aluminum stabilizer for weight reduction.

For the spherical torus-based fusion rocket (STR) to operate continuously and at high-power output, it will be necessary to remove the nonfusionable thermalized charged particle ash (protons and He^4 ions) from the plasma. The magnetic bundle

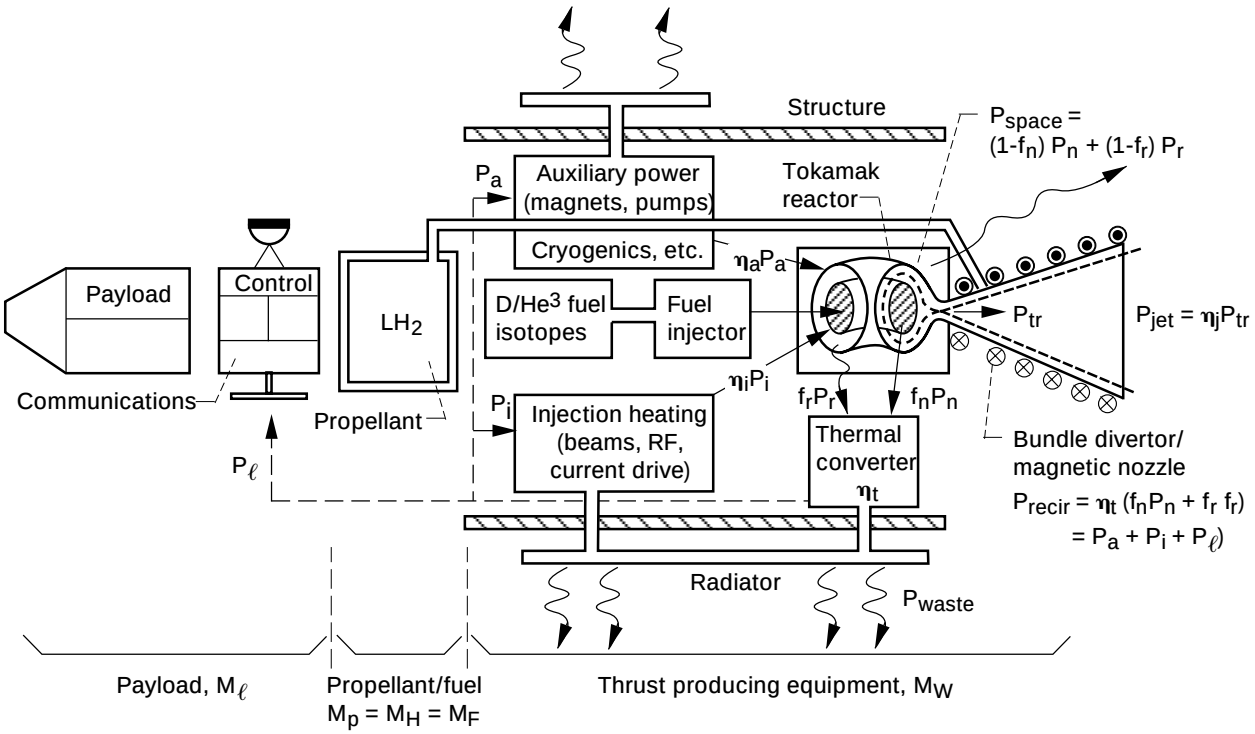

Figure 4.—Component and power flow diagram for an advanced tokamak fusion rocket.[21]

diverter[22] will be an important component for the STR, for it serves as a conduit for channeling plasma exhaust (including wall-generated impurities) out of the torus and into a magnetic field expander (nozzle) where the perpendicular plasma energy can be converted to directed energy along the nozzle axis.

Preliminary estimates[21] indicate that a STR burning a 50/50 fuel mixture of spin polarized DHe^3 could generate ~7500 MW of fusion power, ~6000 MW of which is transport power and the remainder being bremsstrahlung and synchrotron radiation. The neutron producing DD side reactions are assumed to be suppressed. The major radius, plasma elongation, and aspect ratio are 2.48 m, 3.0, and 2.0, respectively leading to a plasma volume of 227 m^3. The toroidal field on the axis (at R_o) and at the center conductor (R_c) are 8.9 and 10.0 T with paramagnetism accounting for a factor of 2 enhancement in B_t. The plasma current is ~86 MA and the volume-averaged fuel ion density and temperature of $\sim 5\times10^{20}$ m^{-3} and 50 keV result in a volume-averaged beta value of ~30%. The overall spacecraft weight is estimated to be ~1033 t and leads to a specific power of α_p ~5.75 kW/kg (assuming $P_{jet} = P_{tr}$).

Spheromak Compact Toroid

Compact toroids (CTs) are axisymmetric plasma configurations in which the toroid is not linked by toroidal magnetic field coils or walls. Theoretically, the CTs offer the improved confinement associated with more complex toroidal geometries, but in a simple, open-ended reactor embodiment with natural diverter action. In such a configuration charged plasma can be exhausted for thrust directly, without the need for a complex bundle diverter for particle extraction.

The spheromak compact toroid (Fig. 5) is a low-aspect-ratio ($A \simeq 2$) plasma configuration which, like the tokamak, uses toroidal (B_t) and poloidal (B_p) magnetic fields for confinement. In the spheromak, however, the poloidally directed currents generating B_t flow in the plasma itself and not in external toroidal field (TF) coils as in the conventional and advanced ST tokamak concepts. Although the TF coils are eliminated in the spheromak, the outward hoop force associated with the toroidal current must be supported by an externally applied "solenoidal" magnetic field (B_e) (equivalent to the vertical magnetic field in a conventional tokamak). An external plasma generator is also required to provide the initial toroidal and poloidal magnetic flux in the spheromak during startup.

In addition to having a simpler coil/blanket geometry, the maximum field strength at the external coils of a spheromak is about half the field value at the plasma center, rather than twice, as in a tokamak. The result is that the spheromak has an engineering beta value $\beta_{eng} \simeq (4\,\mu_o\,nkT/B^2_{coil})$, that is ~15-20 times larger than in a conventional tokamak. Furthermore, because the fusion power density (P_f/V_p) scales like $\beta^2_{eng}\,B^4_{coil}\,\langle\sigma v\rangle/T_i^2$ [Eq. (4)], the spheromak can in principle operate at power densities ~225–400 times higher than in a conventional tokamak for given value of B_{coil} and T_i. By increasing the applied magnetic field to $B_{coil} \simeq 10$ T and exploiting the 40% engineering beta capability[23] of the spheromak, the advanced fusion fuels Cat-DD and DHe^3 can be burned at appreciable power densities. Because typical tokamak and spheromak discharges consist of a hot-interior core, surrounded by a cooler plasma mantle, the volume-averaged density ($\langle n\rangle$) and density-weighted, volume-averaged temperature ($\langle\hat{T}\rangle = \langle nT\rangle/\langle n\rangle$) must be used to correctly evaluate the plasma performance.

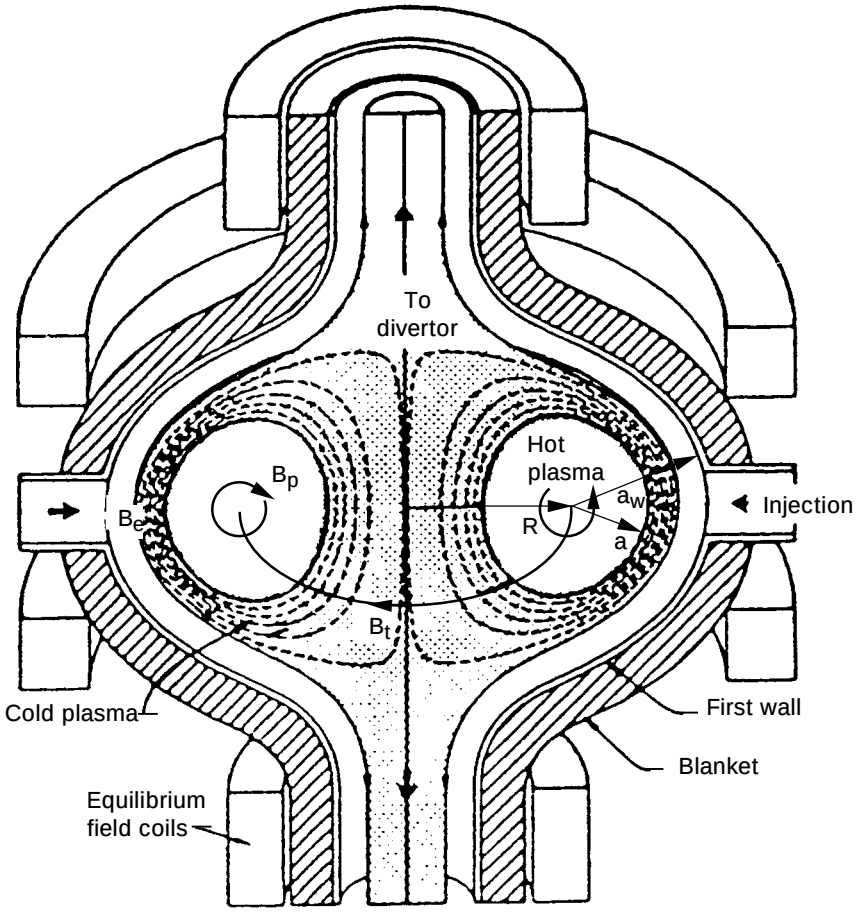

Figure 5.—High β potential and natural divertor action of the spheromak concept can be exploited for rocket thrust.[19]

Here $\langle n \rangle = n_o/(1 + \delta_n)$, n_o and δ_n being the peak density on axis and density-profile shape factor, respectively, and $\langle \hat{T} \rangle = T_o/[(1 + \delta_n + \delta_T)/(1 + \delta_n)]$, δ_T being the temperature profile shape factor. Rewriting Eq. (2) in the following form:

$$\beta_{eng} B_{coil}^2 = 5\mu_o k \langle nT \rangle = 10^{-21} \langle n \rangle \langle \hat{T} \rangle \qquad (5)$$

and specifying $\langle \hat{T} \rangle = 50$ keV, one finds that $\langle n \rangle \simeq 8 \times 10^{20}/m^3$ (assuming flat profiles, i.e, $\delta_n = \delta_T = 0$) and $P_f/V_p \approx 25$ MW/m^3 for a 50/50 DHe^3 mixture [Eq. 3]. Spin polarization of the DHe^3 fuel can increase the power density by a factor of ~1.5, and density, and temperature profile peaking ($\delta_n = 1$, $\delta_T = 2$) by an additional factor of 2 yielding a final fusion power density of ~75 MW/m^3. Assuming the same power level used in the STR ($P_f = 7500$ MW), the spheromak with its higher power density requires a plasma volume ($V_p = 2\pi^2$ Aa^3) of only ~100 m^3 (as compared to ~227 m^3 for the STR). Preliminary calculations indicate that the overall spacecraft weight can be reduced by a factor of ~2.

The higher toroidal field [B_t (R_o) $\simeq$ 20 T] in the $A = 2$ spheromak case considered here leads to an increase in the synchrotron radiation power output ($\propto B_t^2$ nT) but a decrease in the bremsstrahlung output ($\propto n^2 T^{1/2}$) because of the smaller plasma volume. With ~5500 MW available for jet power (assuming $P_{jet} = P_{tr}$), the specific power is estimated to be α_p ~10.5 kW/kg.

Lastly, the spheromak reactor will need very efficient current drive (about several amps per watt of sustaining current drive power) due to the large toroidal and poloidal currents in the device, ~70 and 270 MA, respectively. It is possible that preferential biasing of in situ synchrotron radiation[24] and the bootstrap effect caused by radial diffusion[25] can drive all or a substantial portion of the required currents in the spheromak during steady-state operation. Without an effective means to sustain the internal currents, the magnetic fields will decay providing resistive plasma heating on a magnetic diffusion time scale given by

$$\tau_{mag}(s) \simeq 10[a(m)]^2 [T(keV)]^{3/2} \qquad (6)$$

For $T \sim 50$ keV and $a \sim 1.36$ m, this decay time is long at ~1.8 h. Pulsed operation (with burn times of ~1/2 τ_{mag}) could be a possible option for the spheromak, as well as the spherical torus fusion rocket engines.

Inertial Confinement Fusion Rocket

In the magnetic confinement concepts already discussed, the fuel must be maintained at fairly low density (~10^{20}–10^{21}/m^3) due to β and magnetic field strength limitations. As a result, confinement times of a second or more are required in order to get a substantial burnup of the fuel. In the inertial confinement fusion approach,[26] the requirements on density and confinement time are reversed. Here, multimegajoule pulses (~10 ns in duration) of photons or ions from a driver are used to ablate off the outer surface of a fuel pellet (see Fig. 6). Spherical rocketlike reaction forces implode the remaining fuel to stellar densities (~10^3–10^4 × solid density) while simultaneously heating the central core of the pellet, with a radius comparable to the range of a DT alpha particle (~0.3 g/cm^2), to thermonuclear ignition temperatures (~10 keV). As the fuel burns, the energy generated is used to heat and ignite more fuel. A thermonuclear burn wave driven by α particle self-heating propagates radially outward through the compressed fuel. Compared to the disassembly time of the pellet ($\tau_D \sim R_c/C_s$, R_c and C_s being the compressed pellet radius and ion sound speed, respectively), the fuel reacts so rapidly (<10^{-12} s) that it is confined by its own inertia.

Although magnetic fusion research has been ongoing for the last three decades, the less developed inertial confinement approach to fusion offers the possibility of more compact, lower weight propulsion systems. This is due to the absence of heavy superconducting coils in the primary reactor. By exploiting the high-repetition rates (~10–100 pulses/s) and gain possibilities of ICF, an inertial fusion rocket (IFR) can operate, in principle, at very high-power levels (tens to hundreds of gigawatts) which would be extremely difficult if not impossible to achieve with continuous drive magnetic confinement fusion.

For an ICF system to produce usable quantities of fusion power, the initial investment of driver energy (E_{driver}) must be efficiently coupled into the pellet (E_{fuel}/ε_d, ε_d being the driver energy coupling efficiency) and multiplied during fuel burnup to produce an attractive energy gain ($E_{fusion} = G\,E_{driver}$). The driver energy which effectively couples to the pellet must be capable of 1) isentropically compressing[27] the fuel load to densities on the order of a kilogram per cubic centimeter and 2) igniting the pellet's central core. This energy investment is characteristically quite large, on the order of several megajoules. Because large driver energies usually correspond to high driver weight, there is strong incentive to design high-gain targets (~1000) which can maximize the fusion power output per pulse. The fuel loading in these pellets, however, is usually quite small. In a practical target design the fractional burnup f_b of the fuel is expected to be ~30–50% (substantially higher than in magnetic systems).

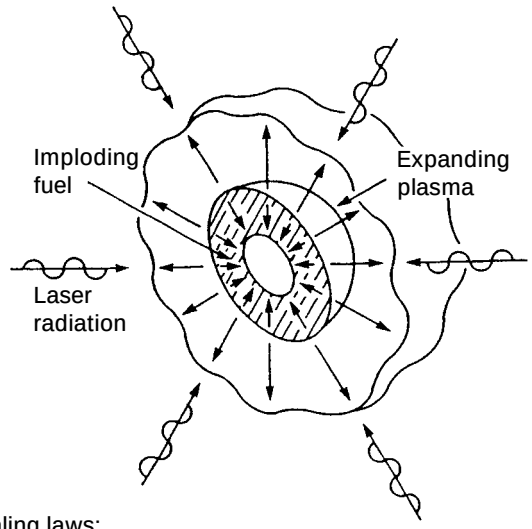

Scaling laws:

$$\left.\begin{aligned}\tau_E = \tau_D \sim \frac{R_c}{C_s}\\ n_j = \rho/\bar{m}_j\end{aligned}\right\} => n\tau_E \sim \rho R/\bar{m}_j C_s$$

Energy balance:

$$E_{fusion} = GE_{driver} = \frac{G}{\varepsilon_D} E_{fuel}\ (\text{thermal})$$

Figure 6.—High-fuel density ρ, energy gain G, and coupling efficiency ε_d are necessary components of inertial confinement fusion.

Assuming the use of deuterium fuel (specific energy of 345 MJ/mg), a target yield of ~2000 MJ will require a fuel loading in the compressed pellet of

$$m_c(\text{mg}) = \frac{E_{fusion}(= 2000\ \text{MJ})/\ 345\ \text{MJ/mg}}{f_b(\sim 40\%)} \approx 15\ \text{mg}$$

Because of the tiny amount of mass involved, the energy release is in the form of a small and potentially manageable explosion. The initiation of a sustained series of these fusion microexplosions within an axially asymmetric magnetic mirror is the essence of inertial fusion rocket propulsion. The thrust of the spacecraft would be produced by redirecting the charged plasma debris from the microexplosion through the larger of the mirror loss cones and out the rear of the vehicle (see Fig. 7).

Hyde[28] has performed a detailed analysis of an IFR which uses two 2-MJ, 6% efficient high-temperature (~1000 K) krypton fluoride (KrF) lasers (each operating at 50 Hz) as the driver. With slightly tritium-enriched deuterium as fuel and a high gain target (G = 1000), the fusion power output consisted of ~1280 MJ of charged plasma power [consistent with the charged particle

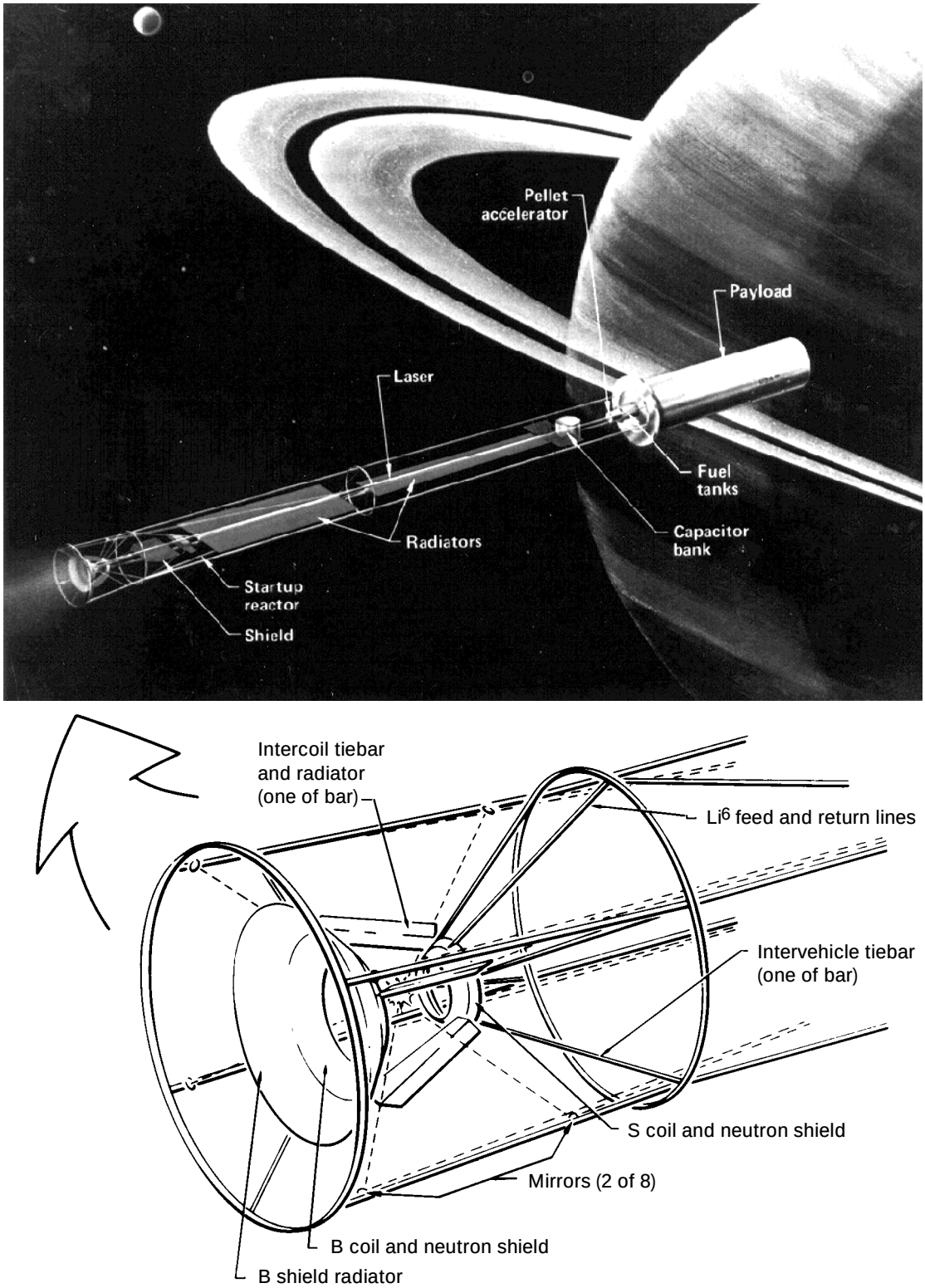

Figure 7.—Inertial confinement fusion rockets capable of higher specific power and impulse operation than their magnetic counterparts could make rapid solar-system-wide travel feasible.[28]

fraction (~60%) of the Cat-DD fuel cycle] and ~710 MJ in the form of x-ray and neutron radiation. Additional propellant mass (~10 times that of the fuel loading) surrounds the pellet providing the ablative material and also augmenting the engine's propulsive thrust. The exhaust velocity (v_{ex}) and jet power are given by

$$v_{ex} = g_o I_{sp} = \eta_j \sqrt{2\, E_{cp}/m_p} \tag{7}$$

and

$$P_{jet} = 1/2 m_p \nu v_{ex}^2 = \eta_j^2 \nu E_{cp} \tag{8}$$

where η_j is the efficiency of the magnetic nozzle in converting charged particle fusion energy E_{cp} to jet energy, m_p is the initial pellet mass (10 x m_c) and ν is pellet repetition rate. With ν = 100 Hz and η_j = 65%, the exhaust velocity and jet power are estimated to be ~2650 km/s (I_{sp} ~ 270 ks) and ~53 GW, respectively. The corresponding thrust level ($F = m_p \nu v_{ex}$) ~40 kN (~ 4 t). The total weight of the engine system was estimated to be ~486 t (~54% of which is attributed to the driver system and ~34% to the magnetic thrust chamber). Based on the given parameters, the specific power of the IFR is α_p = 110 kW/kg.

Antiproton Propulsion System Designs

By exploiting the concepts and technologies currently being examined for use in fission and fusion rocket engines, MARs with a wide range of mission performance capability may be possible. The effectiveness of tungsten (mp 3683 K) in stopping both the decay γ's and the charged pions (range ~9 cm and slowing down time ~0.5 ns) has led to the consideration of a simple heat exchanger concept[2,6] for an antiproton propulsion system. This configuration is equivalent to the solid core fission rocket engines developed during the NERVA nuclear rocket engine program.[8]

In the NERVA engine criticality requirements limited the choice of construction materials to those with low-neutron-capture characteristics. These same requirements also dictated the minimum core size and weight. In the antiproton version of the nuclear thermal rocket, criticality requirements are no longer an issue. The tungsten core is sized to ensure stoppage of most of the annihilation products while providing adequate hydrogen flow for cooling. Using antihydrogen fuel as the energy source, the tungsten core heat exchanger could run to higher operating temperatures than NERVA (>3000 K), resulting in an I_{sp} ~ 1000 s. Preliminary calculations by Howe[6] indicate that a tungsten cylinder, sized to stop most of the annihilation products, would be slightly smaller than the nuclear reactor core designed for the small nuclear rocket engine (SNRE) shown in Fig. 8. The core is compact (~80 cm diameter/80 cm length) and lightweight (~5000 kg assuming 36% void fraction for coolant flow). Calculations also show that significant quantities of neutrons are produced in the core resulting from $\bar{p}$ interactions with heavier nuclei. Howe has sized a $\bar{p}$-NERVA engine for use in a manned Mars mission. The engine would have a thrust of ~4.4×10^5 N (10^5 lbf), a power level of ~2700 MW, engine mass near 7000 kg, and a I_{sp} of ~1100 s. Assuming a 100% deposition of annihilation energy within the tungsten cylinder and ~88.5% conversion efficiency to jet power ($P_{jet} = P_{MA}\eta_j$) leads to

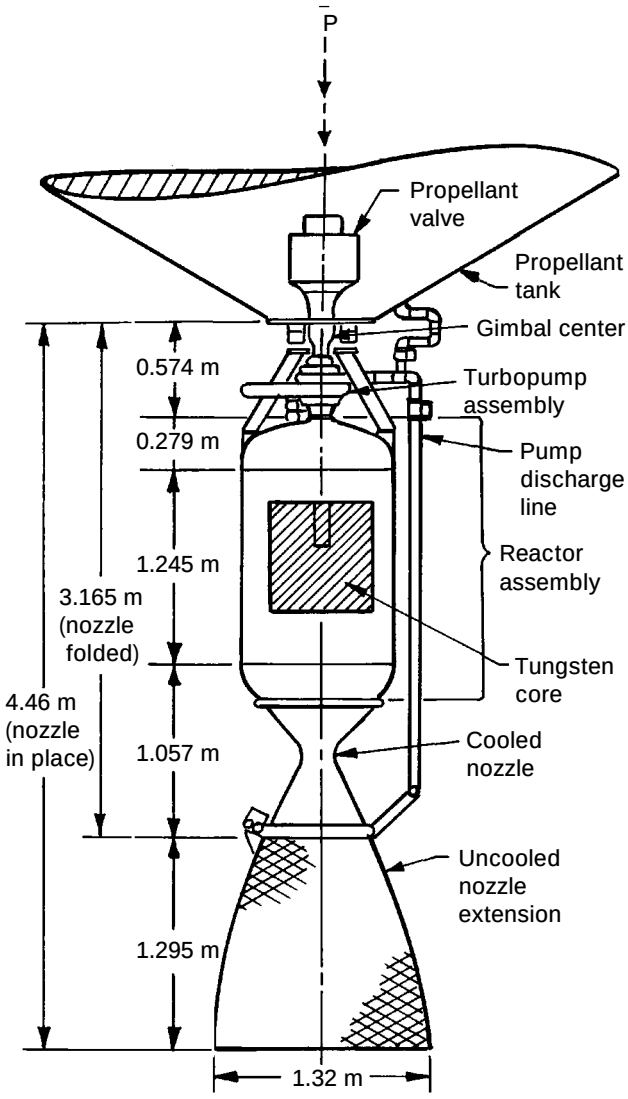

Figure 8.—Schematic diagram of the small nuclear rocket engine designed during the NERVA program; nuclear reactor core replaced with a possible configuration of the metal honeycomb used to convert the antimatter annihilation energy into heat.[6]

$$P_{\mathrm{MA}}(\mathrm{MW}) = P_{\pi^0} + P_{\pi^+} + P_{\pi^-} \simeq 1.8\times10^{8}\dot{m}_{\bar{p}}(\mathrm{g/s})$$

$$\simeq 5.44\times10^{-5}\dot{m}_{p}(\mathrm{kg/s})I_{sp}^{2}(\mathrm{s}) \qquad (9)$$

and corresponding mass flow rates for the antiprotons $\dot{m}_{\bar{p}}$ and hydrogen propellant $\dot{m}_p$ of ~15 μg/s and ~41 kg/s, respectively. For a fission thermal rocket operating at the same parameters, the corresponding burnup of uranium–235 would also be small at ~33 mg/s [~12.2×10^{-6} P_{rx} (MW) g/s]. In both cases the required mass of the nuclear fuels are insignificant compared to the hundreds of metric tons of hydrogen propellant which would be required for a typical Mars mission (discussed in Sec. IV). It is also important to consider the weights of the electric and/or magnetic field devices required for storage, extraction, and injection of the antihydrogen fuel into the tungsten core. These are critical features in concept feasibility and are seldom discussed in the weight estimates of antiproton propulsion systems. The high-temperature benefits of using tungsten can also be exploited in a fission thermal rocket by using tungsten-184 as the structural material. Whereas normal tungsten is quite poisonous to thermal neutrons (having a thermal neutron absorption cross section $\sigma_a \approx 19.2$ b), tungsten-184 has a low absorption cross section ($\sigma_a \approx 2.0$ b) (Ref. 29) and would be suitable for thermal reactor construction. Tungsten-184 comprises about 30% of natural tungsten and would require separation techniques comparable to those used in uranium enrichment facilities. A study[30] made in 1961 indicated the feasibility of enriching tungsten in the 184 isotope using the existing Oak Ridge gaseous diffusion plant equipment with little modification. For production rates of ~27 t per year the cost was estimated to be ~$3500/kg for 93% enrichment. Although increasing the cost of the fission core, the higher operating temperature of tungsten would lead to the same performance characteristics as that of the antimatter system and without the complexities of antimatter handling.

The Gaseous Core Antimatter Rocket

The temperature limitations imposed on either the fission or antiproton solid core thermal rocket designs by the need to avoid material meltdown can be overcome by allowing the core material to exist in a plasma state. In the gaseous-core fission rocket concept,[31] a high-temperature (~25,000–100,000 K) ball of fissioning plasma dissipates its energy ($P = n_u\sigma_f\phi Q_f V_p$) in the form of black-body radiation ($P = \alpha T^4_{\mathrm{rad}} A_s$) which is absorbed by the hydrogen propellant and exhausted as jet power (P = 1/2 $\dot{m}_p v_{\mathrm{ex}}^2$ [= 2 $c_p T_c$]). The parameters, as they appear in order, refer to the uranium atom number density, neutron fission cross section and flux, energy release, plasma volume, the Stefan–Boltzmann constant [= 5.67×10^{-8} W/(m^2)(K^4)], the plasma surface temperature and area, the propellant flow rate, the exhaust velocity of the hydrogen, specific heat, and rocket chamber temperature.

The coaxial flow or open-cycle gas core rocket is illustrated in Fig. 9. It is basically spherical in shape and consists of an outer pressure vessel, a neutron reflector/moderator region, and finally an inner porous liner. A relatively high pressure (~500–1000 atm) is required in the GCR to have a critical mass. Hydrogen propellant, ducted through the outer reactor shell, is injected through the porous wall with a flow distribution that creates a stagnant nonrecirculating central fuel region in the cavity. A small amount of fissionable fuel (~1/4 –1% by mass of the hydrogen flow rate) is exhausted, however, along with the heated propellant. Because ~7–10% of the reactor power is deposited in the reactor shell in the form of high energy gamma and neutron radiation, the I_{sp} capability of the GCR is determined by the cooling capability of the incoming hydrogen propellant. For the regeneratively cooled GCR, the maximum I_{sp} is ~3000 s (Ref. 32). The addition of an external space radiator allows for cooling of the reactor walls and moderator without using up the regenerative cooling capacity of the liquid hydrogen. A factor of 2 increase in I_{sp} (to ~6000 s) is expected for these radiator-cooled systems.

The gas-core reactor concept could also provide a possible configuration for an antimatter rocket which would not have the performance limitations of the solid tungsten system. In the antimatter version of Fig. 9, the critical uranium plasma assembly would be replaced by a high-pressure tungsten gas/plasma capable of absorbing the annihilation debris resulting from the interaction of the injected antihydrogen with the tungsten nuclei. The transfer of annihilation energy to the working hydrogen propellant would again be achieved by radiative means. The ball of tungsten plasma, however, must exist in the minimum of a magnetic well which has sufficient field strength to trap most of the charged pions and follow-on decay products. Whereas some magnetic confinement would also exist for the partially ionized tungsten plasma, the primary method for isolating the tungsten plasma from the hydrogen propellant would be the hydrodynamic technique already discussed. The magnet systems can be of two types (see Fig. 10), but both create a magnetic well in which the field strength increases in all directions away from the center of the device. This configuration is stable against the interchange instability[33] which occurs in simple mirrors whose field lines bulge outward. In this geometry any outward displacement of plasma pressure (even at very low values) weakens the magnetic container and leads to an accelerated plasma loss.

For a maxwellian energy distribution, simple mirror theory provides an estimate of the fraction of charged particles trapped within the magnetic well. This trapping fraction is given by[34]

$$f_T = \left(\frac{R_m - 1}{R_m}\right)^{1/2} = \left(1 - \frac{B_{\min}}{B_{\max}}\right)^{1/2} \qquad (10)$$

where $B_{\min}$ is the magnetic field strength in the mirror well, $B_{\max}$ the value at the mirror peaks, and R_m ($\equiv B_{\max}/B_{\min}$) the

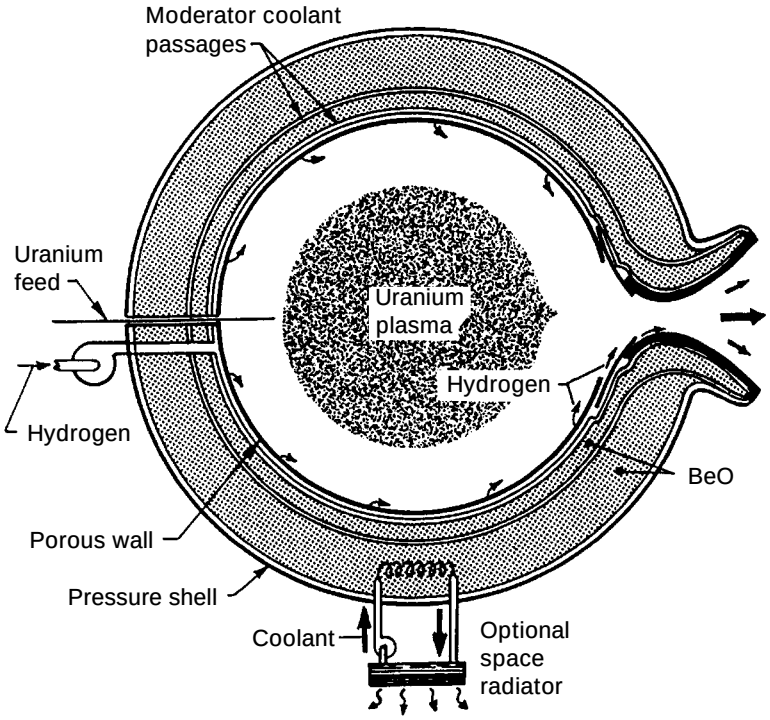

Figure 9.—With the material limits of a solid core removed, the coaxial flow gas core engine could provide high thrust/high I_{sp} operation.[31]

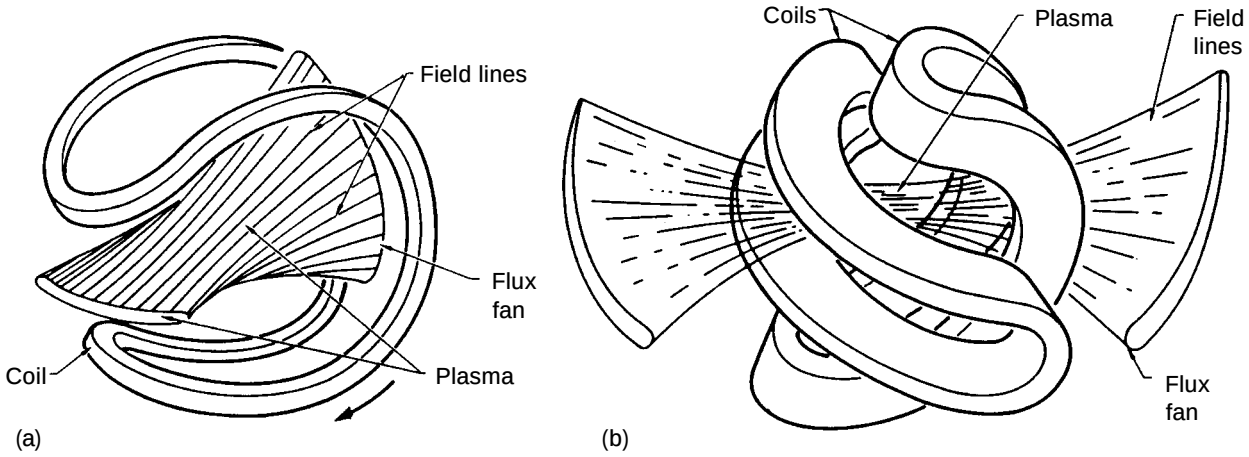

Figure 10.—Sketch of magnet systems used to create a magnetic well for charged particle confinement. (a) Baseball coil. (b) Yin-yang coil geometries.[37]

mirror ratio. Because of the constancy of magnetic moment ($\mu \equiv 1/2\ mv_{\perp}^2/B = W_{\perp}/B$) and conservation of energy ($W = W_{11} + W_{\perp}$), charged particles moving into a region of increasing magnetic field experience a retarding force ($F_Z = -\mu \nabla_Z B$) which reflects them back into the magnetic well. Those particles with $W \approx W_{11}$ have an increased probability of escaping the mirror trap. This probability, expressed in terms of mirror ratio, is given by

$$P = 1 - \left[\frac{R_m - 1}{R_m} \right]^{1/2} \tag{11}$$

and reduces to $P \approx 1/(2\,R_m)$ for moderately large R_m. Cassenti[16] has estimated the fraction of pions trapped within the central region of a magnetic mirror device using the energy distribution of the pions resulting from the annihilation process. Because the

results are only ~3% smaller than those obtained using a maxwellian distribution, the simple estimates provided by Eq. (10) appear adequate.

To illustrate the characteristics of a possible magnetically assisted antimatter GCR, we assume its performance is comparable to that of a reference gas core fission rocket system[32] having the following parameters: P_{rx} = 1500 MW, P_{jet} = 1080 MW, $F = 4.4\times10^4$ N, I_{sp} = 5000 s, M_W = 70 t, $\alpha_p \simeq$ 15 kW/kg, D_c = 2.4 m, $\Delta_{\text{mod}} \simeq 0.8$ m, $T_{\text{rad}} \simeq 1225$ K and $V_f/V_c \simeq 25\%$. The parameters D_c, Δ_{mod}, T_{rad}, and V_f/V_c refer to the diameter of the reactor cavity, the moderator thickness, radiator temperature, and fuel-to-cavity volume ratio, respectively.

To estimate the field requirements for pion trapping we assume the tungsten plasma has the same approximate volume as the fission system. We also specify that $r_{\text{gyro}} \simeq 1/3R_f$ (to ensure adequate confinement of the annihilation debris within the tungsten). For a field strength in the magnetic well of $B_{\text{min}} \simeq 5$ T and a mirror ratio of 3 (corresponding to $f_{T\pi} \simeq 82\%$), the mirror field $B_{\text{max}} \simeq 15$ T. This field level requires the use of niobium-tin (Nb_3Sn) superconductor which has a maximum or critical current density of ~65 kA/cm^2 at ~15 T. And although the pion trapping fraction is high, there is still a substantial energy drain from the system attributed to neutrinos produced during decay of the unstable pions and muons.

Cassenti[16] has examined an antimatter-energized, magnetically assisted hydrogen thermal rocket for orbit transfer vehicle (OTV) applications. His analysis, which assumes 100% loss of gamma power, indicates that ~35% of the remaining annihilation energy can be transferred to the propellant. In the reference fission GCR 10% of P_{rx} reaches the solid, temperature-limited portions of the engine (moderator, etc.) whereas the remaining 1350 MW is converted to jet power assuming an isentropic nozzle expansion efficiency of ~80%. The propellant flow rate is $\dot{m}_p \simeq 0.9$ kg/s. At a specified hydrogen cavity inlet temperature (T_{wa11}) of ~1400 K, the propellant can regeneratively remove 1.2% of the neutron and gamma power ($\dot{m}_p c_p \Delta T \simeq$ 18 MW) with the remaining 8.8% (132 MW) being rejected to space using an external radiator. In the antimatter analog of the GCR we assume that ~1/3 of the annihilation power escapes the tungsten plasma and 50% of the remaining pion energy is radiatively transferred (at an equivalent black-body temperature of ~7555 K) to the surrounding envelope of hydrogen propellant. At ~33% conversion efficiency (consistent with Cassenti's results) the total annihilation power and antiproton fueling rate is ~4050 MW and 22.5 μg/s, respectively.

Because shielding will be required to protect the superconducting magnets from gamma radiation in a real system, it is logical to consider recovery of some portion of gamma power deposited in the shield, and to assess the impact of regenerative cooling on $\bar{p}$ fueling requirements and high I_{sp} operation. Because of its high-temperature capability and good attenuation characteristics against gamma radiation, we consider a tungsten shield/pressure vessel configuration the thickness of which can be determined using

$$I_\gamma(x)/I_\gamma(0) = \exp\left[-\left(\mu_e/\rho\right)\rho x\right] \tag{12}$$

Here $I(x)/I(0)$ is the ratio of the gamma ray intensities [$I(0)$ being the intensity at the shield surface], μ_e/ρ is the material energy absorption coefficient [~0.1 cm^2/g for energetic gamma rays ($E_\gamma > 100$ MeV)] and ρx is the density (19.3 g/cm^3) times shield thickness which is proportional to the weight. For P_γ = 1350 MW and a tungsten thickness of 4 cm, the superconducting magnets see a heat load of ~0.6 MW_t. Because a modern liquid-helium refrigerator requires ~500 W_e of electrical power to remove each watt of heat at 4.2 K and masses ~4 t/kW_t, such a heat load is intolerable for a portable propulsion system. At ~7 cm the heat load is down to ~2 kW_t and can be handled by an 8 t refrigerator with ~ 1 MW of electrical power input.

For the antimatter GCR to operate at the same I_{sp}, propellant flow rate, and hydrogen inlet temperature as its fission counterpart (i.e., 5000 s, 0.9 kg/s and 1400 K) the external radiator must dissipate ~1332 MW of gamma power because only 18 MW can be removed regeneratively by the hydrogen propellant. Assuming a radiator specific mass of ~19 kg/m^2 and operating temperature of ~1225 K, the radiator mass is estimated to be ~193 t [M_{rad} (kg) $\simeq 145\, Q_{\text{rad}}$ (MW) (Ref. 32)]. Increasing the radiator temperature to ~1500 K could reduce this value to 87 t.

Rather than dissipating the gamma power to space, it can be recovered by operating the tungsten at elevated temperatures (~3250 K) and introducing the hydrogen propellant into the reactor cavity at this value. Assuming the same level of jet power ($P_{\text{jet}} = P_{\text{core}}\, \eta_j$ = 1080 MW; η_j = 80%) and 50% conversion of available charged pion energy (1350 MW), the required annihilation power and $\bar{p}$ fueling rate drops by a factor of 2 to 2025 MW and 11.25 μg/s, respectively. To recover the 675 MW of gamma power at 3250 K a propellant flow rate into the cavity of ~14.3 kg/s (a factor of ~16 greater than the 5000 s case) is required which reduces the effective specific impulse to ~1250 s.

Because the regenerative cooling overwhelms the high I_{sp} benefits of the GCR concept, one might consider eliminating the magnetic system entirely and operating the engine in a mode equivalent to that of the liquid core fission rocket (LCR) concept discussed by Rom.[35] Here the liquid fission fuel is held against the outside of a rocket chamber by centrifugal force obtained by spinning the chamber (Fig. 11). After cooling the chamber wall, the hydrogen propellant would be bubbled through the liquid fuel and out the nozzle. In the antimatter version of the LCR, molten liquid tungsten would replace the liquid uranium. A fluid layer ~10 cm in thickness could trap most of the annihilation energy. The higher boiling point of tungsten (~5930 K vs 4091 K for uranium) could lead to a vacuum specific impulse of ~1800–2000 s at a chamber pressure of ~ 10 atms and an exhaust-to-chamber pressure ratio of 10^{-3} (Ref. 36). The

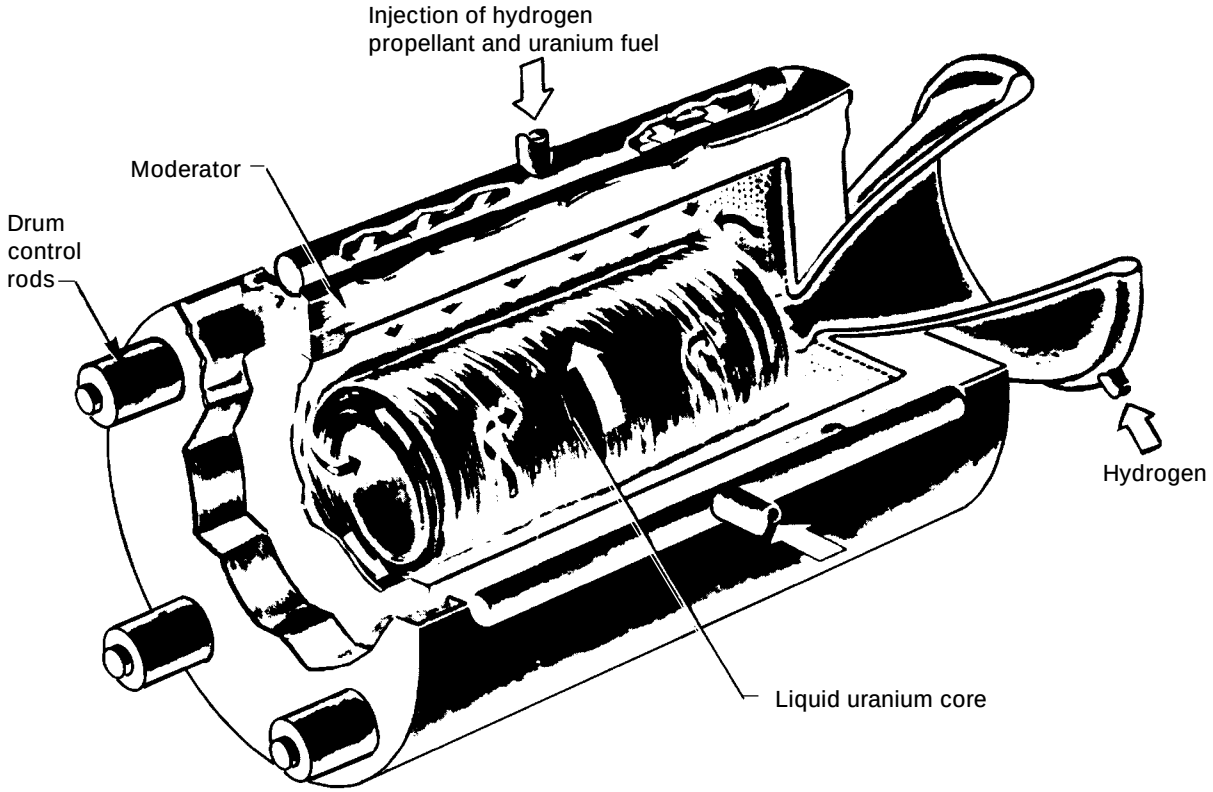

Figure 11.—Schematic of a liquid core fission rocket engine.

corresponding I_{sp} for the fission LCR is ~1300–1500 s for the same conditions. Over this I_{sp} range the F/M_W ratio is estimated to be ~2–10.[35] The limits on the fission LCR are attributed to increased vaporization of the nuclear fuel with increasing temperature and its subsequent entrainment in the hydrogen propellant which decreases the effective I_{sp}. One can assume similar difficulties with the antimatter LCR as the boiling-point temperature of tungsten is approached. However, with a F/M_W ~2 and an I_{sp} of ~2000 s, the specific power is quite attractive at ~190 kW/kg vs ~145 kW/kg for the fission LCR with the same F/M_W and an I_{sp} = 1500 s.

By contrast, the 5000 s gaseous core systems have substantially lower thrust-to-engine weight ratios. At a thrust level of 44 kN and M_W ~70 t [major components being the moderator (28 t), radiator (19 t) and pressure vessel (23 t)], the F/M_W ratio is $\simeq 6.4 \times 10^{-2}$ for the fission GCR. For the antimatter system the weight of the tungsten shield/pressure vessel is estimated to be ~25 t assuming a cavity radius of 1.2 m and a vessel thickness of ~7 cm. We estimate the weight of the SC magnet by scaling the yin-yang coil design (see Fig. 10b) used in the mirror fusion test facility (MFTF).[37] The MFTF contains copper stabilizer (~8.9 t/m^3) and niobium-titanium (NbTi) superconductor (~6.4 t/m^3) cooled to 4 K by liquid helium. The magnet dimension is ~3 m between mirror points and the maximum field is ~7 T. The coil weight is ~150 t. For our application the magnet dimension is ~1/2 that of MFTF (at 1.5 m) but $B_{max} \simeq 15$ T. Using an aluminum stabilizer (~2.7 t/m^3) and vanadium-gallium (V_3Ga) superconductor (~6.1 t/m^3) with a 70% packing fraction (the remaining 30% of the coil cross sectional area containing coolant and structure), the coil weight is estimated to be ~70 t. Together with the radiator mass (estimated at 87 t for T_{rad} = 1500 K), the total engine weight is ~182 t. This results in a F/M_W ratio of ~2.5×10^{-2} and a specific power of ~5.9 kW/kg, a factor of 2.5 lower than that of the fission GCR.

Antiproton Heated Magnetically Confined Plasma Rockets

In the antimatter version of the GCR the magnetic mirror system was used to confine the energetic pions, muons and electrons and to improve collisional dissipation of the annihilation energy into the tungsten plasma. As a next logical step one might consider using fusion type magnetic confinement systems to contain a plasma working fluid which is energized by injecting antiprotons into the magnetic bottle. If operated in a steady-state mode the energetic plasma could be extracted using either a magnetic bundle divertor (for closed toroidal magnetic geometries, such as the tokamak) or the natural divertor action of the compact toroids, such as the spheromak. Assuming for

simplicity that the specific impulse of a hydrogen plasma rocket is given by

$$I_{sp}(s) = \frac{1}{g_o}\sqrt{\frac{3kT_H}{m_H}} \simeq 1.73\times 10^3\left[T_H(\text{eV})\right]^{1/2} \qquad (13)$$

then I_{sp} in the range of 5,000–15,000 s should be possible with plasma exhaust temperatures of ~10–50 eV (1 eV = 1.16×10^4 K). From Eq. (2) the maximum plasma density that can be confined will depend on the available magnetic field strength and the β capability of the particular confinement concept. Assuming β = 50% and B = 15 T, the achievable densities are

$$n_e(\text{cm}^{-3}) \simeq \begin{cases} 1.5\times10^{19} & \text{for } T_e = 10 \text{ eV} \\ 3.0\times10^{18} & \text{for } T_e = 50 \text{ eV} \end{cases}$$

The ability to sustain the preceding plasma characteristics using an antiproton heating source can be determined using a simple plasma power balance

$$2/3\,P_{MA}/V_p = \left\{P_{\text{ion}} + P_{cx} + P_{\text{rad}} + P_{\text{tr}}\right\}/V_p \qquad (14)$$

which neglects the gamma power component. The sink terms on the right refer to losses due to ionization of cold hydrogen gas, charge exchange of cold neutrals with warm ions, various radiation mechanisms and collisional diffusion processes.

At sufficiently high-ionization levels (which exist for $T_e \geq$ 10 eV) the neutral hydrogen density is low and ionization and charge exchange losses can be neglected to first order. Impurity radiation losses can also be ignored if one assumes a pure hydrogen plasma. Under these conditions bremsstrahlung radiation will be the primary nondiffusive energy loss mechanism. Bremsstrahlung (or braking) radiation is emitted when rapidly moving charged particles–mainly electrons—undergo a sudden deflection as a result of a near collision with a plasma ion. For a pure hydrogen plasma the bremmstrahlung power loss per unit volume is given by[38]

$$\frac{P_{\text{brems}}}{V_p}\left(\frac{\text{MW}}{\text{m}^3}\right) = 5.35\times10^{-43}\left[n_e(\text{m}^{-3})\right]^2\left[T_e(\text{keV})\right]^{1/2} \qquad (15)$$

Because of the strong density scaling, the bremsstrahlung power loss increases from ~10^6 to 1.2×10^7 MW/m^3 as the density increases from 0.3 to 1.5×10^{19}/cm^3. These levels are ~10^6 to 10^7 times larger than those found in typical fusion plasmas (with n_e ~5×10^{14}/cm^3 and T_e ~20 keV). At sufficiently high densities and low temperatures, however, it is possible for the plasma to reabsorb the emitted photons. The approximate mean free path for a bremsstrahlung photon in a hydrogen plasma is given by[39]

$$\lambda(\text{cm}) \simeq 10^{48}\left[T_e(\text{keV})\right]^{3.5} \Big/ \left[n_e(\text{cm}^{-3})\right]^2 \qquad (16)$$

Equation (16) assumes that the photon frequency ν is given by $h\nu = kT_e$ where h is Planck's constant (= 6.626×10^{-34} J/s). At T_e = 10 eV and $n_e = 1.5\times10^{19}$ cm^{-3}, λ ≃ 4.5 m. This distance increase to ~30 km for T_e = 50 eV and $n_e \simeq 3\times10^{18}$ cm^{-3}. It is only at very low temperatures (≤5 eV) that adequate reabsorption occurs (e.g., λ ≃ 2 cm for $T_e \simeq 2$ eV and $n_e \simeq 1.5\times10^{19}$ cm^{-3}). The need to prevent excessive bremmstrahlung emissions through low-temperature operation leads to performance characteristics for the plasma rocket which are roughly equivalent to those found in the gas and liquid core versions of the antimatter rocket described earlier.

Even assuming that adequate reabsorption can occur at higher temperatures it is difficult for relativistic charged particles to slow down via plasma collisional effects. Consider a relativistic test particle with velocity V_T slowing down in a maxwellian plasma consisting of electrons and ions having thermal velocities V_{Te} and V_{Ti}. In the limiting case of $V_T > V_{Te} >> V_{Ti}$, the slowing down time is given (in cgs units with T in eV) by[40]

$$\tau_s(s) \simeq \frac{m_T^2 V_T^3}{4\pi n_e e^2 q_T^2 (2 + m_T/m_e)\ln\Lambda} \qquad (17)$$

where m_T and m_e are the masses of the test particle and electron, respectively, q_T is the charge of the test particle, and ln Λ is the coulomb logarithm. For relativistic particles slowing is mainly due to scattering off of electrons. The slowing down time is also longer for heavier test particles implying that a charged pion ($m_\pi \simeq 273.5m_e$) will take longer to slow down than a muon ($m_\mu \simeq 206.5m_e$). For an average pion kinetic energy of 250 MeV, $V_T = V_\pi = c\,(\gamma^2 - 1)^{1/2}/\gamma \simeq 93.3\%c$, $q_T^2 = e^2$, $m_T \simeq 2.492\times10^{-25}$g and ln Λ ≤ 5 (assuming $n_e \simeq 1.5\times10^{19}$ cm^{-3} and $T_e \simeq 10$ eV), resulting in an average slowing down time of ~100 μs (almost 1500 times longer than the pion's relativistic lifetime of ~70 ns). Under such conditions the pions would decay into muons coupling little of their energy into the plasma. The muons, in turn, would have a slowing down time of ~75 μs (assuming an average kinetic energy of ~193 MeV, $q_T^2 = e^2$, $m_T \simeq 1.882\times10^{-25}$g and $V_T \simeq 93.5\%c$) which is over 10 times their relativistic lifetime of ~6.2 μs. The stable electrons and positrons (with an average kinetic energy of ~100 MeV) would slow down in ~0.2 μs. Assuming all of their energy can be coupled to the plasma only ~18% (Ref. 14) of the annihilation would be available for propellant heating.

For fusion plasmas with $V_{Ti} < V_T < V_{Te}$, τ_s is given by[40]

$$\tau_s(\mathrm{s}) = m_T^2 \Big/ \left\{ 4\pi n_e e^2 q_T^2 \left[\frac{Z}{V_T^3}\left(1+\frac{m_T}{m_i}\right) + \frac{4}{3\sqrt{\pi}}\left(1+\frac{m_T}{m_e}\right)\left(\frac{m_e}{2kT_e}\right)^{3/2} \right] \ln\Lambda \right\} \qquad (18)$$

Both the electrons and ions contribute to slowing in a fusion plasma and a colder plasma can slow the test particles more quickly. For example, a 14.7 MeV proton (Z = l) produced in a DHe^3 plasma operating at $n_e \simeq 7.5\times10^{14}$ cm^{-3}, $T_e \simeq 50$ keV, and $\ln\Lambda \simeq 17.5$ would slow down in ~525 ms. This is less than the characteristic energy confinement time of approximately several seconds which exists for most magnetic fusion reactors.

The preceding results indicate that stable fusion products are more effective in coupling their reaction energy into the bulk plasma than are the unstable pions and muons. Because of the poor coupling in an antimatter plasma rocket ~50% of annihilation energy could be lost in neutrinos. The 33% of the annihilation energy that appears as gamma power must be either dissipated via a heat rejection system (at the cost of additional spacecraft weight) or recovered regeneratively.

Some recovery seems prudent from an economics standpoint since an 18% conversion factor will require a factor of 5 increase in the amount of antihydrogen required for a given operating power level.

Mission Performance Characteristics

Traditionally propulsion systems have been characterized as either high-thrust/ specific impulse-limited systems (such as chemical and nuclear fission rockets) or low-thrust/power-limited-systems (such as fission electric rockets). The antimatter systems we have discussed fit into the first category having flight profiles characterized by short burning periods separated by long coast periods. The fusion systems, however, provide a unique third category of engine capable of high thrust/high I_{sp} operation and fast interplanetary travel.

Antimatter Systems

In assessing the performance potential of the antimatter systems we have selected round-trip travel to Mars as the candidate mission. Simple estimates of the total velocity impulse (ΔV) for such a mission has been provided by Irving and Blum[41] as a function of the round-trip travel time in months (see Fig. 12). The four separate velocity increments, ΔV_1, ΔV_2, ΔV_3, ΔV_4, are those required for Earth escape, Mars capture, Mars escape, and Earth capture, respectively. By using the equations describing the system mass ratio ($R_M = M_i/M_f = \exp[\Delta V/g_o I_{sp}]$; i and f denoting the initial and final mass of the spacecraft) and jet power ($P_{jet} = 1/2\ \dot{m}_p[g_o I_{sp}]^2$), the total engine burn time [t(s) = M_p (kg)/ $\dot{m}_p$(kg/s)] can be expressed (in mks units) in the following form:

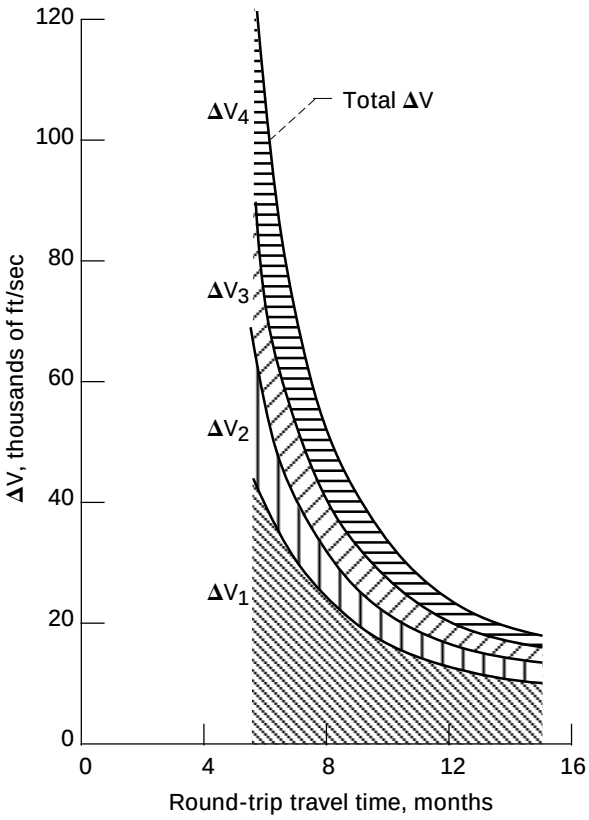

Figure 12.—Total velocity impulse required for round trip ballistic travel to Mar.[41]

$$t_b = \frac{g_o^2}{2}\frac{I_{sp}^2}{P_{jet}}\left(M_W + M_L\right)\left(\exp\left[\Delta V/g_o I_{sp}\right] - 1\right) \qquad (19)$$

The parameter M_i (= $M_W + M_L + M_P = M_f + M_p$) is the initial spacecraft mass in Earth orbit and is composed of a propulsion system mass M_W, a payload mass M_L, and a propellant mass M_P. The dry mass of the spacecraft is denoted by M_f.

A 6 month quick trip ($\Delta V \simeq 30.5$ km/s) and a 1 year round-trip mission ($\Delta V \simeq 7.6$ km/s) to Mars have been selected as the candidate missions. Using Eq. (19) and its supporting equations,

the system mass ratio, total engine burntime, and total propellant requirements have been estimated. The antiproton and uranium fuel inventories required for the mission have also been calculated along with an estimated fuel cost based on 5 M$/mg for antihydrogen[5] and ~ 50 k$/kg for enriched uranium. A summary of the performance characteristics for solid, liquid, and gaseous core antimatter systems, and their fission analogs, is found in Table 3. The solid and liquid core systems assume a thurst level of 10^5 lbf (~4.45×10^5N) and the GCR systems a value 1/10th of that at 10^4 lbf (~4.45×10^4N). The 6-month Mars mission is difficult for both the $\bar{p}$ and U^{235} versions of the NERVA engine. It requires large propellant loadings and substantial quantities of antihydrogen at significant cost. Payload delivery costs to low Earth orbit dominate total mission costs, however, and amount to ~$5.6 billion (5.6 B$) and ~10.4 B$ for the $\bar{p}$ and U^{235} systems, respectively, assuming a Saturn V-class launch vehicle with launch costs of ~$3300/kg (~$1500/lbm). For the fission option the uranium fuel costs are low, requiring an investment of ~$12 million (M$) for the engine's critical fuel mass (M_{crit}) estimated at ~0.1 kg per megawatt of reactor power output ($P_{rx} = P_{jet}/\eta_j$).

The 582 mg of antihydrogen required for the Mars quick trip by the $\bar{p}$ NERVA concept can be reduced by optimizing the system specific impulse for minimum antihydrogen usage.[42] Minimum use is achieved when $I_{sp} = 0.63\,\Delta V/g_o \simeq 1960$ s. The antimatter LCR concept operates near optimum conditions and could potentially perform the 6-month Mars mission with an initial mass in Earth orbit (IMEO) of ~474 t. The fission version of the LCR limited to an I_{sp} of ~1500 s due to enhanced fuel vaporization has a higher IMEO (~795 t). The F/M_W was specified at ~3.2 for the LCR systems (half the value in the $\bar{p}$ NERVA system) because of the need for a thick external moderator/reflector necessary to ensure neutron economy in the fission system. The radiator-cooled gas core fission rocket

Table 3 Summary of antimatter and fission engine performance

ΔV, km/s	R_M	t_b, h	M_p, t	$M_{\bar{p},u}$, mg/kg	Launch/Fuel costs
$\bar{p}$ NERVA: P_{jet} = 2386 MW, I_{sp} = 1100 s, $\dot{m}_p$ = 41 kg/s, $\dot{m}_{\bar{p}}$ 15 μg/s, $M_W + M_L$ = 100 t					
30.5	16.9	10.8	1590	582	5.6 B$/2.9 B$
7.6	2.02	0.69	102	37	0.7 B$/0.2 B$
NERVA: P_{jet} = 1963 MW, I_{sp} = 900 s, $\dot{m}_p$ = 50.4 kg/s, $M_u = M_{crit}$ kg, $M_W + M_L$ = 100 t					
30.5	31.7	16.9	3066	222	10.4 B/$ 11.7 M$
7.6	2.37	0.76	137.9	222	0.8 B$/11.7 M$
$\bar{p}$ LCR: P_{jet} = 4362 MW, I_{sp} = 2000 s, $\dot{m}_p$ = 22.7 kg/s, $\dot{m}_{\bar{p}}$ = 26.1 μg/s, $M_W + M_L$ = 100 t					
30.5	4.74	4.58	374	430	1.6 B$/2.2 B$
7.6	1.47	0.58	47.4	54.5	0.5 B$/0.3 B$
Fission LCR: P_{jet} = 3267 MW, I_{sp} = 1500 s, $\dot{m}_p$ = 30.2 kg/s, $M_u = 4\,M_{crit}$ kg, $M_W + M_L$ = 100 t					
30.5	7.95	6.39	695	1400	2.6 B$/70 M$
7.6	1.68	0.63	68.5	1400	0.6 B$/70 M$
$\bar{p}$ GCR: P_{jet} = 1080 MW, I_{sp} = 5000 s, $\dot{m}_p$ = 0.9 kg/s, $\dot{m}_{\bar{p}}$ = 22.5 μg/s, $M_W + M_L$ = 282 t					
30.5	1.86	75.0	243	6075	1.7 B$/30.4 B$
7.6	1.17	14.8	48.0	1199	1.1 B$/6.0 B$
Fission GCR: P_{jet} = 1080 MW, I_{sp} = 5000 s, $\dot{m}_p$ = 0.9 kg/s, $M_u = \dot{m}_u t_b$ + 100 kg, $M_W + M_L$ = 170 t					
30.5	1.86	45.2	146	830	1.0 B$/41.5 M$
7.6	1.17	8.94	29.0	245	0.7 B$/12.3 M$

offers the best performance of all the $\bar{p}$ and fission systems examined. Because the GCR engine featured here is an open cycle design,[32] a quantity of U^{235} fuel ($\dot{m}_u/\dot{m}_p \sim 0.5\%$) is exhausted from the engine along with the hydrogen propellant. Added to this amount of lost U^{235} are four critical core loadings (each at ~25 kg) required for the four major propulsion maneuvers. The $\bar{p}$ GCR suffers from very high-fuel costs attributed to the larger engine weight (~182 t vs 70 t for fission GCR) and the poorer coupling of the annihilation products to the working fluid.

Fusion Systems

High-power fusion rockets possess the best attributes of both fission thermal engines (prolonged operation at relatively high thrust) and the fission-powered electric propulsion systems (high I_{sp}). It is envisioned that the fusion spacecraft would depart from and return to geosynchronous Earth orbit (GEO). In traveling between planetary bodies, the sun is considered to be the only source of gravitational force. Because the initial acceleration levels for the fusion systems examined here range from ~3–5×10^{-3} g_o (mg_o) (compared to the sun's gravitational pull of ~0.6 (mg_o) straight line trajectories can be assumed. To illustrate the performance potential for the fusion systems we have considered one-way and round-trip continuous burn acceleration/deceleration trajectory profiles which assume constant I_{sp}, F, and P_{jet} operation. The equations describing the transit times for the outbound and return legs of a journey from A to B (and back again) along with the distances traveled are given by[21]

$$\tau_{AB}(\mathrm{s}) = \frac{I_{sp}(\mathrm{s})}{F/W_f}\left(\frac{1}{\beta}\right)\left(\frac{1}{\alpha}-1\right) \tag{20}$$

$$\tau_{BA}(\mathrm{s}) = \frac{I_{sp}(\mathrm{s})}{F/W_f}\left(\frac{1}{\beta}-1\right) \tag{21}$$

$$\tau_{RT}(\mathrm{s}) = \tau_{AB} + \tau_{BA} = \frac{I_{sp}(\mathrm{s})}{F/W_f}\left(\frac{1}{\alpha\beta}-1\right) \tag{22}$$

$$D_{AB}(\mathrm{m}) = \frac{g_o\, I_{sp}^2(\mathrm{s})}{F/W_f}\left(\frac{1}{\beta}\right)\left(\frac{1}{\sqrt{\alpha}}-1\right)^2 = D_{BA} \tag{23}$$

$$D_{BA}(\mathrm{m}) = \frac{g_o\, I_{sp}^2(\mathrm{s})}{F/W_f}\left(\frac{1}{\sqrt{\beta}}-1\right)^2 \tag{24}$$

where $W_f = M_f g_o$ is the dry weight, $1/\alpha = M_i/M_B$ ($M_B = M_f + M_P^{B\to A}$; $M_P^{B\to A}$ being the propellant used in traveling from B to A), $1/\beta \equiv M_B/M_f$, and $R_M = 1/(\alpha\beta)$. By specifying a particular planetary mission and its distance from Earth (1 astronomical unit (AU) = 1.495×10^{11} m), Eqs. (23) and (24) can be used to determine $1/\alpha$ and $1/\beta$ and their product, the spacecraft mass ratio. By knowing the mass of the thrust producing system (M_W) and specifying a payload mass (M_L) the IMEO, propellant requirements, and trip times can be calculated. Assuming a planetary refueling capability, Eqs. (21) and (24) can also be used to calculate one-way results. In this case $R_M = 1/\beta$.

The performance characteristics for a spherical torus, spheromak and inertial fusion rocket are summarized in Tables 4–6. Table 4 indicates that with planetary refueling possible, the STR can journey to Mars in ~34 days. The IMEO

Table 4 Spherical torus fusion rocket performance

STR characteristics

Polarized DHe^3, I_{sp} = 20 ks, $\dot{m}_p$ = 0.308 kg/s, α_p = 5.75 kW/kg, M_W = 1033 t, M_L = 200 t

One-way continuous burn/constant I_{sp} trajectory profile:

Mission[a]	D_{AB}, AU	R_M	M_i, t	M_p, t	M_L/M_i, %	τ_{AB}, days	a_i, 10^{-3} g_o
Mars	0.524	1.732	2135	902	9.4	33.9	~2.9
Ceres	1.767	2.497	3079	1846	6.5	69.4	2.0
Jupiter	4.203	3.590	4427	3194	4.5	120.0	~1.4

Round-trip trajectory results:

Mission[a]	R_M (= $1/\alpha\beta$)	$M_p^{A\to B}$	$M_p^{B\to A}$	$M_p^{A\to A}$	M_i	τ_{AB}	τ_{BA}	τ_{RT}
Mars	2.664	1149	902	2051	3284	43.2	33.9	77.1
Ceres	4.667	2675	1846	4521	5754	100.5	69.4	169.9
Jupiter	7.783	5169	3194	8363	9596	194.3	120.0	314.3

[a]Closest approach distances to Earth.

Table 5 Spheromak fusion rocket performance
SFR characteristics

Polarized DHe^3, I_{sp} = 50 ks, $\dot{m}_p = 4.95\times10^{-2}$ kg/s, $\alpha_p \simeq 11.5$ kW/kg, M_W = 515 t, M_L = 200 t

Round-trip continuous burn/constant I_{sp} trajectory profile:

Mission[a]	D_{AB}, AU	R_M	M_i, t	M_p, t	M_L/M_i, %[b]	τ_{AB}, days	τ_{RT}, days
Mars	0.524	1.465	1047	332	19.1	40.6	77.6
		(1.222)	(872)	(157)	(23.0)	(36.7)	– – –
Ceres	1.767	1.923	1375	660	14.5	83.2	154.0
Jupiter	4.203	2.55	1823	1108	11.0	114.4	258.7

[a]Closest approach distance to Earth.
[b]For outbound leg of journey.

Table 6 Inertial Fusion Rocket Performance
IFR characteristics

Cat-DD, I_{sp} = 270 ks, $\dot{m}_p$ = 0.015 kg/s, α_p = 110 kW/kg, M_W = 486 t, M_L = 200 t

Round-trip continuous burn/constant I_{sp} trajectory profile:

Mission[a]	D_{AB}, AU	R_M (= $1/\alpha\beta$)	M_i, t	$M_p^{A\to A}$, t	M_L/M_i, %[b]	τ_{AB}, days	τ_{RT}, days
Mars	0.524	1.104	757.3	71.3	26.4	27.7	55.0
Ceres	1.767	1.196	820.5	134.5	24.4	53.1	103.7
Jupiter	4.203	1.309	898	212.0	22.3	84.6	163.6
Saturn	8.539	1.453	997	311.0	20.1	125.5	239.8
Uranus	18.182	1.689	1159	473.0	17.3	194.1	364.7
Neptune	29.058	1.901	1304	618.0	15.3	257.3	476.9
Pluto	38.518	2.063	1415	729.0	14.1	306.6	562.7

[a]Closest approach distances to Earth.
[b]For outbound leg of journey.

is 2135 t of which ~42% is propellant, 9.4% is payload and 48% is engine. The initial acceleration level is ~3 mg_o which is 5 times the value of the sun's gravitational pull at Earth. Jupiter can also be reached in ~4 months with a propellant loading of ~3200 t. Without a planetary refueling capability, the spacecraft must carry along sufficient propellant for the return trip. This requirement increases the overall IMEO and mission duration. The spheromak being lighter can operate at reduced propellant flow rates and higher specific impulse and still maintain initial acceleration levels of several milligees. With the SFR round-trip missions to Jupiter of ~8.5 months are possible with an IMEO ~1823 t and with a payload mass fraction of over 10%. (In all of the results shown, it is assumed that an equivalent amount of payload is returned.) The SFR can also perform one-way missions to Mars in ~37 days with initial mass requirements under 875 t (results shown in parentheses).

The STR and SFR results assumed the use of spin polarized DHe^3 in order to eliminate neutron radiation and obtain a lighter spacecraft. If the benefits of spin polarized DHe^3 are not achievable, magnetic fusion engines can still burn deuterium but at the expense of increased mass. By exploiting the high repetition rate and target gain possibilities of inertial confinement fusion, the IFR can not only burn abundant deuterium fuel efficiently, but it can do so with a relatively lightweight engine system (<500 t) (see Table 6). And whereas MCF rockets can reach out into the solar system by employing planetary refueling, the IFR can perform round-trip missions to Pluto (carrying a 200 t payload) in ~18.5 months (no refueling required). The IMEO would be 1415 t with propellant and payload mass fractions of ~52% and ~14%, respectively. We know of no other advanced propulsion concept with this capability. Tritium would be bred onboard the spacecraft to facilitate ignition of the DD fuel pellets and the deuterium fuel load

which comprises ~10% of the propellant inventory would cost ~73 M$ at current prices of ~$\$10^3$/kg.

Conclusions

The purpose of this chapter has been to compare various antimatter and fusion rocket concepts in an effort to obtain a clearer understanding of the advantages and disadvantages associated with each system. The areas examined have included fuel cycle characteristics, physics and technology requirements, mission performance capability, and fuel cost and availability issues. A number of subject areas have not been addressed. These include the antiproton reactivity issue at elevated temperatures, methods for injecting antiprotons into high-pressure gas/plasma reaction chambers, the effect of pion–nucleon collisions on slowing down, and the assumption of lightweight systems for the storage, extraction, and injection of antiprotons. All of these issues are expected to be important in the realization of a working anitmatter system.

On the basis of preliminary results obtained thus far, antimatter thermal rockets utilizing solid and liquid fission core reactor concepts offer the potential for high-thrust (~4.5×10^5 N)/high I_{sp} (up to ~2000 s) operation. The antimatter liquid core engine is capable of 6-month round-trip missions to Mars with IMEO <500 t and a system mass ratio of ~4.75 close to the optimum value of 4.9 obtained for minimum antihydrogen usage. The fuel costs are still large, however, because of the substantial IMEO requirements for the Mars mission. Furthermore, the $\bar{p}$ LCR is outperformed by the radiator-cooled, fission GCR in terms of IMEO, launch and fuel costs which brings into question the rationale for developing the more complex $\bar{p}$ system.

The coupling of the annihilation energy contained in the relativistic charged particles appears more difficult in high-temperature gaseous or plasma working fluids. Because high-field (>10 T) superconducting coils will be needed to improve energy coupling, they must be heavily shielded to minimize the power and mass requirements of the refrigeration system. In addition to a substantial radiation shield and magnet mass, an antimatter gas core design would require a large space radiator to dissipate unwanted gamma-ray power. Regenerative cooling of the shield/pressure vessel configuration requires a significant propellant flow rate into the cavity due to the large gamma power component. This quickly overwhelms the high I_{sp} feature of the gaseous core concept.

By contrast, fusion rocket engines burning the advanced fusion fuels Cat-DD or DHe^3 produce mainly stable hydrogen and helium reaction products which quickly thermalize in the bulk plasma. The bremsstrahlung power loss, which is emitted primarily in the soft x-ray photon range, can also be readily handled in a lightweight shield/blanket configuration and used to generate recirculating power for the system. The energetic particles which collisionally diffuse out of the plasma can be exhausted directly at high I_{sp} (<10^5 s) or mixed with additional hydrogen for thrust augmentation. Magnetic fusion engines with specific powers in the range of 2.5–10 kW/kg and I_{sp} of 20,000–50,000 s could enable round-trip missions to Jupiter in less than a year. Inertial fusion rockets with α_p >100 kW/kg and $I_{sp} > 10^5$ s offer outstandingly good performance over a wide range of interplanetary destinations and round-trip times. Even Pluto is accessible with round-trip travel times of less than 2 years. Finally, whereas synthetic antihydrogen must be manufactured, stable fusion fuels are found in abundance throughout the solar system (particularly the outer gas planets). Fusion rockets employing planetary refueling at selected locations (e.g., Mars, Callisto, and Titan) could open up the entire solar system to human exploration and colonization.

References

1. Morgan, D.L., "Investigationa of Matter Antimatter Interaction for Possible Propulsion Applications," NASA CR–141356, 1974.
2. Forward, R.L., "Antiproton Annihilation Propulsion," *Journal of Propulsion*, Vol. 1, 1985, p. 370.
3. Forward, R.L., "Exotic Propulsion in the 21st Century," Proceedings of the American Astronautical Society, 33rd Annual Meeting, AAS 86-409, Boulder, CO, Oct. 27–29, 1986.
4. North, D.M., "USAF Focuses Development on Emerging Technologies," *Aviation Week and Space Technology*," Vol. 19, Feb. 24, 1986.
5. Forward, R.L., Cassenti, B.N., and Miller, D. , "Cost Comparisons of Chemical and Antihydrogen Propulsion Systems for High DV Missions," AIAA Paper 85-1455, July 1985.
6. Howe, S.D., Hynes, M.V., Prael, R.E., and Steward, J.D. , "Potential Applicability of the Los Alamos Antiproton Research Program to Advanced Propulsion," Proceedings of the 15th International Symposium on Space Technology and Science, LA-UR-86-1689, Tokyo, Japan, May 19–23, 1986.
7. Forward, R.L., "Antiprotron Annihilation Propulsion," Air Force Rocket Propulsion Lab., AFRPL-TR-85-034, Aug. 15, 1985, p. 55.
8. Altseimer, J.H., et al., "Operating Characteristics and Requirements for the NERVA Flight Engine," AIAA Paper 70-676, June 1970.
9. Ragsdale, R.G., "To Mars in 30 Days by Gas-Core Nuclear Rocket," *Astronautics and Aeronautics*, Vol. 65, Jan. 1972.
10. McNally, J.R., Jr., "Physics of Fusion Fuel Cycles," *Nuclear Technology/Fusion*, Vol. 2, Jan. 1982, p. 9.
11. Wittenberg, L.J., Santarius, J.F., and Kulcinski, G.L., "Lunar Source of He^3 for Commercial Fusion Power," *Fusion Technology*, Vol. 10, Sept. 1986, p. 167.

12. Kulsrud, R.M., Furth, H.P., Valeo, E.J., and Goldhaber, M., "Fusion Reactor Plasmas with Polarized Nuclei," *Physics Review Letters*, Vol. 49, 1982, p. 1248.
13. Adyasevich, B.P., and Fomenko, D.E., "Analysis of Investigation of the Reaction D(d,p)T with Polarized Deuterons," *Soviet Journal of Nuclear Physics*, Vol. 9, 1969, 167.
14. Cassenti, B.N., "Design Consideration for Relativistic Antimatter Rockets," AIAA Paper 81-1531, July 1981.
15. Morgan, D.L., "Concepts for the Design of an Antimatter Annihilation Rocket," *Journal of the British Interplanetary Society*, Vol. 35, 1982, 405.
16. Cassenti, B.N., "Antimatter Propulsion for OTV Applications,'' AIAA Paper 84-1485, June 1984.
17. Barkas, W.H., and Berger, M.J., "Tables of Energy Losses and Ranges of Heavy Charged Particles," NASA SP-3013, 1964.
18. Peng, Y.-K.M., Strickler, D.J., Borowski, S.K., et al., "Spherical Torus: An Approach to Compact Fusion at Low Field - Initial Ignition Assessments," ANS 6th Top. Mtg. on Tech. of Fusion Energy, San Francisco, CA, March 1985.
19. Katsurai, M., and Yamada, M., "Studies of Conceptual Spheromak Fusion Reactors," *Nuclear Fusion*, Vol. 22, 1982, 1407.
20. Bernabei, S., et al., "Lower-Hybrid Current Drive in the PLT Tokamak," *Physics Review Letters*, Vol. 49, 1982, 1255.
21. Borowski, S.K., "A Physics/Engineering Assessment of a Tokamak-Based Magnetic Fusion Rocket," AIAA Paper 86-1759, June 1986.
22. Stott, P.E., Wilson, C.M. and Gibson, A., *Nuclear Fusion*, Vol. 17, 1977, 481; and *Nuclear Fusion*, Vol. 18, 1978, 475.
23. Yamada, M., "Review of Experimental Spheromak Research and Future Prospects," *Fusion Technology*, Vol. 9, 1986, 38.
24. Dawson, J.M., and Kaw, P.K., "Current Maintenance in Tokamaks by Use of Synchrotron Radiation," *Physics Review Letters*, Vol. 48, 1982, 1730.
25. Bickerton, R.J., Connor, J.W., and Taylor, J.B., "Diffusion Driven Plasma Currents and Bootstrap Tokamak," *Nature, Physics Science*, Vol. 229, 1971, 110.
26. Duderstadt, J.J., and Moses, G.A., *Inertial Confinement Fusion*, Wiley, New York, 1982.
27. Nuckolls, J., Wood, L., Thiessen, A., and Zimmerman, G., "Laser Compression of Matter to Super-High Densities: Thermonuclear (CTR) Application, *Nature*, Vol. 239, 1972, 139.
28. Hyde, R., "A Laser Fusion Rocket for Interplanetary Propulsion," 34th International Astronautical Conf., AIF Paper 83-396, Budapest, Hungary, Oct. 1983.
29. Rom, F.E., "Fast and Moderated Reactors and Applications of Low-Power Nuclear Rockets," *Nuclear, Thermal and Electric Rocket Propulsion*, edited by R.A. Willaume, A. Jaumotte and R.W. Bussard, Gordon and Breach Science, New York, 1967, p. 162.
30. Rom, F.E., "Fast and Moderated Reactors and Applications of Low-Power Nuclear Rockets," *Nuclear, Thermal and Electric Rocket Propulsion*, edited by R.A. Willaume, A. Jaunotte, and R.W. Bussard, Gordon and Breach Science, New York, 1967, p. 75.
31. Ragsdale, R.G. , "Gas-Core Rocket Reactors—A New Look," AIAA Paper 71-641, June 1971.
32. Ragsdale, R.G., "High-Specific-Impulse Gas-Core Reactors," NASA TM X-2243, NASA/Lewis Research Center, March 1971.
33. Rosenbluth, M.N., and Longmire, C.L., *Annals of Physics*, 1957, 1120.
34. Glasstone, S., and Lovberg, R.H., *Controlled Thermonuclear Reactions*, D. Van Nostrand, Princeton, NJ, 1960, p. 336.
35. Rom, F.E., "Nuclear Rocket Propulsion, NASA/Lewis Research Center, TM X-1685, Cleveland, OH, 1968.
36. King, C.R., "Compilation of Thermodynamic Properties, Transport Properties, and Theoretical Rocket Performance of Gaseous Hydrogen," NASA/Lewis Research Center, NASA TN D-275, Cleveland, OH, April 1960.
37. Post, R.F., "Experimental Base of Mirror-Confined Physics," *Fusion*, edited by E. Teller, Academic Press, New York, Vol. 1, Pt. A, 1981, p. 430.
38. Glasstone, S., and Lovberg, R.H., *Controlled Thermonuclear Reactions*, D. Van Nostrand, Princeton, NJ, 1960, p. 31.
39. Glasstone, S., and Lovberg, R.H., *Controlled Thermonuclear Reactions*, D. Van Nostrand, Princeton, NJ, 1960, p. 28.
40. Krall, N.A., and Trivelpiece, A.W. , *Principles of Plasma Physics*, McGraw-New York, 1973, pp. 302–303.
41. Irving, J.H., and Blum, E.K., "Comparative Performance of Ballistic and Low Thrust Vehicles for Flights to Mars," *Vistas in Astronautics*, Vol. 11, Pergamon Press, New York, 1959, p. 191.
42. Shepherd, L.R., "Interstellar Flight," *Journal of the British Interplanetary Society*, Vol. 11, 1952, pp. 149–167.

REPORT DOCUMENTATION PAGE

Form Approved
OMB No. 0704-0188

1. AGENCY USE ONLY (*Leave blank*)	2. REPORT DATE	3. REPORT TYPE AND DATES COVERED
	March 1996	Technical Memorandum

4. TITLE AND SUBTITLE

Comparison of Fusion/Antiproton Propulsion Systems for Interplanetary Travel

5. FUNDING NUMBERS

WU–242–10–01

6. AUTHOR(S)

Stanley K. Borowski

7. PERFORMING ORGANIZATION NAME(S) AND ADDRESS(ES)

National Aeronautics and Space Administration
Lewis Research Center
Cleveland, Ohio 44135–3191

8. PERFORMING ORGANIZATION REPORT NUMBER

E–9712

9. SPONSORING/MONITORING AGENCY NAME(S) AND ADDRESS(ES)

National Aeronautics and Space Administration
Washington, D.C. 20546–0001

10. SPONSORING/MONITORING AGENCY REPORT NUMBER

NASA TM–107030
AIAA–87–1814

11. SUPPLEMENTARY NOTES

Prepared for the 23rd Joint Propulsion Conference cosponsored by AIAA, ASME, SAE, and ASEE, San Diego, California, June 29—July 2, 1987. Responsible person, Stanley K. Borowski, organization code 6850, (216) 977–7091.

12a. DISTRIBUTION/AVAILABILITY STATEMENT

Unclassified - Unlimited
Subject Categories 16 and 20

This publication is available from the NASA Center for Aerospace Information, (301) 621–0390.

12b. DISTRIBUTION CODE

13. ABSTRACT ***(Maximum 200 words)***

Rocket propulsion driven by either thermonuclear fusion or antiproton annihilation reactions is an attractive concept because of the large amount of energy released from a small amount of fuel. Charged particles produced in both reactions can be manipulated electromagnetically making high thrust/high specific impulse (I_{sp}) operation possible. A comparison of the physics, engineering, and costs issues involved in using these advanced nuclear fuels is presented. Because of the unstable nature of the antiproton-proton ($\bar{p}p$) reaction products, annihilation energy must be converted to propulsive energy quickly. Antimatter thermal rockets based on solid and liquid fission core engine designs offer the potential for high thrust (~10^5 lbf)/high I_{sp} (up to ~2000 s) operation and 6 month round trip missions to Mars. The coupling of annihilation energy into a high-temperature gaseous or plasma working fluid appears more difficult, however, and requires the use of heavily shielded superconducting coils and space radiators for dissipating unused gamma ray power. By contrast, low-neutron-producing advanced fusion fuels (Cat-DD or DHe^3) produce mainly stable hydrogen and helium reaction products which thermalize quickly in the bulk plasma. The energetic plasma can be exhausted directly at high I_{sp} ($\simeq 10^5$s) or mixed with additional hydrogen for thrust augmentation. Magnetic fusion rockets with specific powers (α_p) in the range of 2.5 to 10 kW/kg and I_{sp} in the range of 20,000–50,000 s could enable round trip missions to Jupiter in less than a year. Inertial fusion rockets with $\alpha_p > 100$ kW/kg and $I_{sp} > 10^5$s could perform round trip missions to Pluto in less than 2 years. On the basis of preliminary fuel cost and mission analyses, fusion systems appear to outperform the antimatter engines for difficult interplanetary missions.

14. SUBJECT TERMS

Gas core rocket; Fusion propulsion; Antiproton; Nuclear thermal rocket; NTR; Magnetic confinement (MCF); Inertial confinement (ICF)

15. NUMBER OF PAGES

26

16. PRICE CODE

A03

17. SECURITY CLASSIFICATION OF REPORT	18. SECURITY CLASSIFICATION OF THIS PAGE	19. SECURITY CLASSIFICATION OF ABSTRACT	20. LIMITATION OF ABSTRACT
Unclassified	Unclassified	Unclassified	